Master's thesis

NTNU
Norwegian University of Science and Technology
Faculty of Engineering
Department of Civil and Environmental Engineering

Ola Berge

An experimental and numerical study of eccentrically placed rectangular hollow section braces on chords under out-of-plane bending moment

Master's thesis in Civil and Environmental Engineering
Supervisor: Arne Aalberg and Arild Holm Clausen
June 2022

NTNU
Norwegian University of Science and Technology

Ola Berge

An experimental and numerical study of eccentrically placed rectangular hollow section braces on chords under out-of-plane bending moment

Master's thesis in Civil and Environmental Engineering
Supervisor: Arne Aalberg and Arild Holm Clausen
June 2022

Norwegian University of Science and Technology
Faculty of Engineering
Department of Civil and Environmental Engineering

NTNU
Norwegian University of
Science and Technology

Department of Structural Engineering
Faculty of Engineering
NTNU – Norwegian University of Science and Technology

ACCESSIBILITY

Open

MASTER THESIS 2022

SUBJECT AREA:	DATE:	NO. OF PAGES:
Structural mechanics	10.06.2022	41 + 12

TITLE:

An experimental and numerical study of eccentrically placed rectangular hollow section braces on chords under out-of-plane bending moment

En eksperimentell og numerisk studie av eksentrisk plasserte rektangulære hulprofil staver på gurt under ut-av-planet bøyemoment

BY:

Ola Berge

SUMMARY:
This study investigates the moment capacity of braces placed eccentrically onto a chord. Construction of roof and floors may use eccentric braces to save space or material. Due to the eccentricity of the brace placement, the instance loses some of its capacity.

Based on the available literature, only one study on this subject seems to have been performed earlier. The study used chord and brace cross-sections, where only one ratio β=0.67 was considered, where β is the ratio between the height of the brace and chord. In this study, a wider range of β-values is analysed to investigate how the moment capacity changes with changing β-values.

Finite element analyses were performed to investigate the behaviour of structures with centric and eccentrically placed braces. The analyses revealed that the models where the brace is placed eccentric lose capacity compared to those where the brace is placed centric. The analyses also revealed that instances with brace to chord height ratio above 0.80 will have a rotational displacement of the chord face resisted by the corners of the chord, giving those models a larger capacity.

A physical experiment was performed to calibrate the models used in this study properly. Furthermore, the results of the experiment were compared to analyses with equal β-value, ensuring that the finite element analyses can represent physical behaviour.

RESPONSIBLE TEACHER: Arne Aalberg

SUPERVISOR(S): Arne Aalberg, Arild H. Causen

CARRIED OUT AT: Department of Structural Engineering, NTNU

Preface

This masters thesis concludes my five-year Civil and Environmental Engineering study at the Norwegian University of Science and Technology.

By having my own research project, I have been given much knowledge about finite element modelling, steel joints and mechanics. Both the theoretical and physical experience is appreciated and will be put to good use.

I would like to thank my supervisors Arne Aalberg and Arild H. Clausen for their feedback and help over the course of this semester. Your understanding of mechanics and how to approach this problem has been a vital part of the thesis, and could not have been completed without you. Some attention should also be directed to Khashaiar Ashourzadeh at Norconsult for using his freetime to help understanding the problem.

I would also like to thank my parents Liv A. Hatten and Lars Berge for their love and support. Having the possibility to call home and talk to my loves ones made it possible for me to continue the hard work needed to get through this education. I also want to thank my grandparent Evy Berge and Per Berge for opening their home for me, making dinner and making my stay in Trondheim as perfect as possible.

Trondheim, June 10. 2022.
Ola Berge

Abstract

This study investigates the moment capacity of braces placed eccentrically onto a chord. Construction of roof and floors may use eccentric braces to save space or material. Due to the eccentricity of the brace placement, the instance loses some of its capacity.

Based on the available literature, only one study on this subject seems to have been performed earlier. The study used chord and brace cross-sections, where only one ratio β=0.67 was considered, where β is the ratio between the height of the brace and chord. In this study, a wider range of β-values is analysed to investigate how the moment capacity changes with changing β-values.
.

Finite element analyses were performed to investigate the behaviour of structures with centric and eccentrically placed braces. The analyses revealed that the models where the brace is placed eccentric lose capacity compared to those where the brace is placed centric. The analyses also revealed that instances with brace to chord height ratio above 0.80 will have a rotational displacement of the chord face resisted by the corners of the chord, giving those models a larger capacity.

A physical experiment was performed to calibrate the models used in this study properly. Furthermore, the results of the experiment were compared to analyses with equal β-value, ensuring that the finite element analyses can represent physical behaviour.

Sammendrag

Denne studien undersøker momentkapasiteten til sekundærbjelker plassert eksentrisk på en hovedbjelke. Konstruksjoner av tak og gulv kan velge å bruke sekundærbjelker som er eksentrisk plassert på hovedbjelken for å spare plass eller materialer. På grunn av den eksentriske plasseringen av sekundærbjelken, vil konstruksjonen få redusert kapasitet.

Basert på tilgjengelig litteratur ser det ut som det kun er gjennomført en studie på dette temaet tidligere. Studien bruker en hovedbjelke og sekundærbjelke med tverrsnitt som gir størrelsesforhold β=0.67, hvor beta er forholdet mellom høyden til sekundærbjelken og hovedbjelken. I denne studien flere β-verdier testet for å undersøke hvordan momentkapasiteten endrer seg med β-verdiene.

Elementanalyser ble gjennomført for å undersøke oppførselen til konstruksjoner med sentrisk og eksentrisk plassert sekundærbjelke. Analysene avslørte at modeller med eksentrisk plassert sekundærbjelke har mindre momentkapasitet sammenlignet med sentriske plasserte sekundærbjelker. Analysene avslørte i tillegg at i konstruksjoner hvor størrelsesforholdet er over 0.80, vil hovedbjelkens hjørner gjøre motstand mot rotasjon av hovedbjelkens steg og dermed gi økt kapasitet.

Et fysisk eksperiment ble gjennomført for å etterprøve modellene brukt i denne studien. Resultatene av eksperimentet ble sammenlignet med elementmodeller med tilsvarende β-verdi, og viste at elementanalyser kan representere fysisk oppførsel til slike forbindelser.

Content

List of symbols

t_0	Thickness of chord
t_1	Thickness of brace
b_0	Width of chord wall
b_1	Width of brace wall
b_{eff}	Effective width of cross-section
h_0	Height of chord wall
h_1	Height of brace wall
f_{y0}	Characteristic yield stress of the chord
f_{y1}	Characteristic yield stress of the brace
β	Ratio of brace height to chord height
k_n	Factor used in the design of the chord
n	Stress ratio for RHS-members
$W_{pl,1}$	Plastic section modulus for brace
γ_{M5}	Partial safety factor
$\sigma_{0,Ed}$	Maximum stress in the chord at a joint
$M_{op,1,Rd}$	Design value of the resistance of the joint

List of Figures

1 Introduction

Steel is a material with high ductility, strength and durability at a low price. Steel is also easy to form for wanted cross-sections and applications and can be reused without losing characteristics. Steel is an alloy which can be mixed with other elements to add other more properties, like higher strength, be corrosion-resistant or be more ductile. Those properties make steel one of the most used building materials globally. Since the two main ingredients in steel, iron and carbon, can be found globally, steel is easily accessible. Steel structures are steel parts connected through bolts and welds into a monolithic structure. These structures may become very big, and large loads occur in the parts and connections. Hence, connections must have sufficient capacity to resist those loads. Today, most connections used in steel constructions are covered in the Eurocode, but some are missing. When connections are not covered in the Eurocode, a company has to use time and money to analyze the connection properties.

Rectangular hollow sections (RHS) have a high strength to weight ratio, come at a low cost and are aesthetically nice. RHS also has a high capacity in compression, lateral-torsional buckling and bending in all directions compared to open steel cross-sections with similar area and size. Those properties make RHS profiles wanted in many areas of steel structures, especially where the parts are subjected to large loads like columns and different types of frameworks. Another benefit of the RHS is that it can be filled with concrete to increase the static properties. Packer et al. 2009.

1.1 Problem definition

In some floor and roof structures consisting of a framework of chords with braces connecting between, there may be a need to place the braces eccentric onto the chords to save space. Steel structures like this are often subjected to significant loads due to the weight of a concrete floor or roof. Centric placement of the brace onto the chord is covered in EC3, but not the eccentric placement of the brace. In today's building industry, Eurocode is used to calculate the capacity of connections where the brace is placed eccentrically. It is done by calculating the capacity as if the brace is placed centric and changing some variables to fit the stiffest part of the connection. The capacity is then halved, giving the industry a roughly calculated capacity when modelling the construction. This method results in a smaller capacity than it is in reality. The industry uses larger cross-sections and more material to compensate for the capacity loss, resulting in increased use of money. In this thesis, finite element analyses and an experimental test will be performed to investigate how the moment-capacity changes when the brace is placed eccentrically onto the chord compared to centrically placed braces. See figure 1.1.

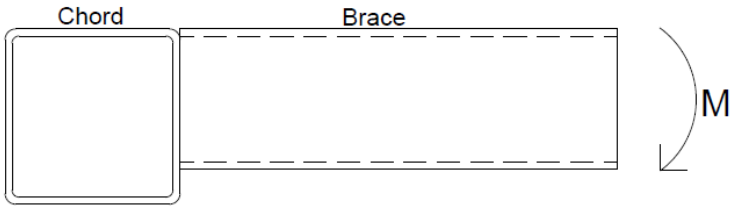

!

Figure 1.1: Out-of-plane bending moment on eccentrically placed brace

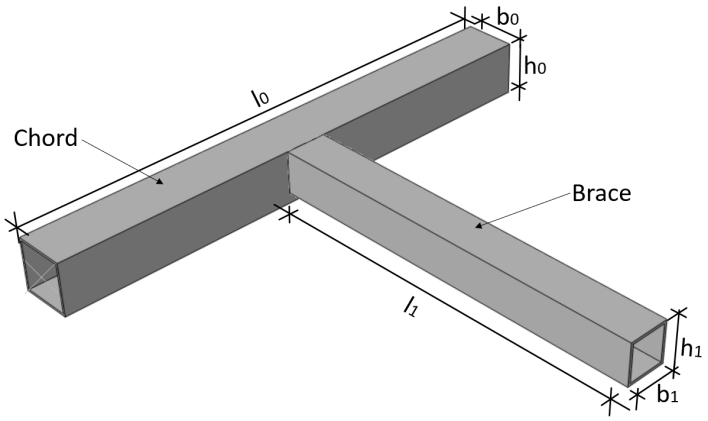

!

Figure 1.2: Chord and Brace geometry

2 Theory

2.1 Material properties

Some material properties is independent from alloys, and thereby is considered universal in the construction industry. Some of the most typical used values is listed in table 1.

Name	Symbol	Typical value
Elastic modulus	E	210000 MPa
Density	ρ	7850 kg/m^3
Poissons ratio	ν	0.3

Table 1: Typical material properties for steel

If there is a linear relationship between the stress and the strain, it is a linear material. Steel is a linear homogenious material, meaning steel has the same properties in both tension and compression. A linear material behaves according to formula 2.1, which is called Hooke's law.

$$\sigma = E\varepsilon \tag{2.1}$$

When a material reaches the yielding stress, the material will start to permanently deform. At this point, Hooke's law is no longer valid since the stress-strain relationship is not linear anymore. Stresses and strains in the plastic area can be calculated using formula 2.2, and 2.3.

$$\sigma_{eng} = \frac{F}{A_0} \tag{2.2}$$

$$\varepsilon_{eng} = \frac{\Delta L}{L_0} \tag{2.3}$$

2.2 Centric placement of brace on chord

NS-EN 1993-1-8 2009 covers joints between hollow sections. Subsection 7.5 covers welded connections between centric RHS brace members and RHS chord members. Table 7.14 gives the design moment resistance of T-joints with out-of-plane moment. What design moment resistance to calculate depends on the β-value of the joint. β is calculated according to formula 2.4.

$$\beta = \frac{h_1}{h_0} \tag{2.4}$$

Chord face failure, $\beta \leq 0.85$

$$M_{op,1,Rd} = k_n f_{y0} t_0^2 \left(\frac{h_1(1+\beta)}{2(1-\beta)} + \sqrt{\frac{2b_0 b_1(1+\beta)}{1-\beta}}\right)/\gamma_{M5} \tag{2.5}$$

Chord side wall crushing, $0.85 < \beta \leq 1$

$$M_{op,1,Rd} = f_{y0} t_0 (b_0 - t_0)(h_1 + 5t_0)/\gamma_{M5} \tag{2.6}$$

Chord distortional failure

$$M_{op,1,Rd} = 2f_{y0} t_0 (h_1 t_0 + \sqrt{b_0 h_0 t_0 (b_0 + h_0)})/\gamma_{M5} \tag{2.7}$$

Brace failure, $0.85 < \beta \leq 1$

$$M_{op,1,Rd} = f_{y1}(W_{pl,1} - 0.5(1 - b_{eff}/b_1)^2 b_1^2 t_1)\gamma_{M5} \tag{2.8}$$

Where k_n and b_{eff} is calculated according to formula 2.14 and 2.11. n is calculated according to formula 2.10

$$k_n = \begin{cases} 1.3 - \frac{0.4n}{\beta} & \text{for } n > 0 \\ 1 & \text{for } n \leq 0 \end{cases} \tag{2.9}$$

$$n = \frac{\sigma_{0,Ed}/f_{y0}}{\gamma_{M5}} \tag{2.10}$$

$$b_{eff} = \frac{10}{b_0/t_0}\frac{f_{y0}t_0}{f_{y1}t_1} b_1, b_{eff} \leq b_1 \tag{2.11}$$

2.3 Moment-rotation study on eccentric placed brace

Zhao et al. 2020 performed a study on the moment-rotation behaviour of eccentric rectangular hollow section type cross-sections under out-of-plane bending moment and chord stress in 2020. The study uses experimental results to validate an FE-model, which is used to investigate how different parameters influence the moment-rotation behaviour of the model. The model used in this study is an x-joint, where the braces are connected eccentrically onto both the chord faces, with a cover plate connecting the top flanges of the braces and a weld connecting it to the top flange of the chord too. Zhao et al. 2020 found that the failure mode for the models is plasticization of the chord face and that the FE-models can represent this behaviour well. A four-parameter exponential function is also developed to describe the moment-rotation relationship with $\beta \leq 0.95$. See equation 2.12.

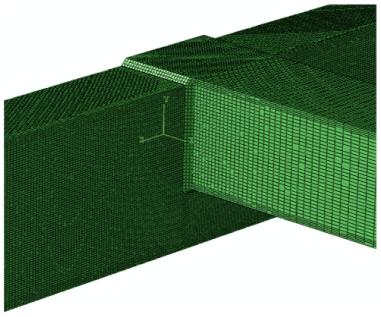

(a) Joint zone of Zhao et al. FE-model

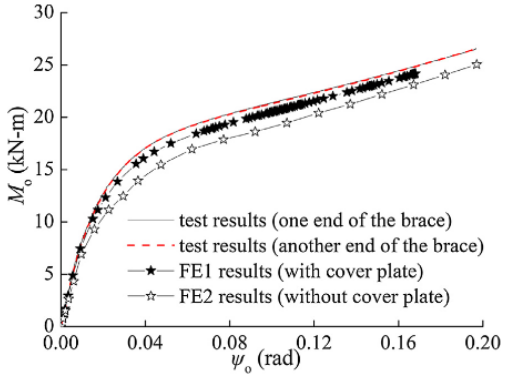

(b) Comparison between FE-analyses and experimental test

Figure 2.1: Figures from Zhao et al. study

$$M_0 = M_{op}(1 - exp[\frac{-(k_{oi} - k_{op} + C\psi_0)\psi_0}{M_{op}}]) + k_{op}\psi_0 \tag{2.12}$$

Where C is a constant, and M_0, k_oi and k_op are defined as follows.

$$M_0 = \begin{cases} 0 & \text{for } \psi = 0 \\ M_{op} + k_{op}\psi_0 & \text{for } \psi_0 \to \infty \end{cases} \tag{2.13}$$

$$\frac{dM_0}{d\psi_0} = \begin{cases} k_{oi} & \text{for } \psi = 0 \\ k_{op} & \text{for } \psi_0 \to \infty \end{cases} \tag{2.14}$$

2.4 Rotation

Rotation means that an object performs circular movement around a centre point or axis. For the setup of this numerical study, there are mainly two elements which rotate. The brace will rotate about the axis following the length of the chord. The

other part rotating is the face of the chord. Compression and tension forces transferred from the brace will displace the chord face where the top and bottom flanges of the brace connect with the chord, giving it a rotational displacement. Since the thesis is investigating the moment-rotational behaviour of the joint, only the rotation of the chord face is used. Gil et al. 2003

In an experimental test, it is hard to measure the rotational displacement of the chord face. Instead, rotational deflection of the brace can be used. To find the rotational displacement of the brace in the joint zone, the deflection of the rigid connected brace, w_{fixed}, must be calculated and subtracted from the total deflection of the brace w_{tot} to get the remaining deflection w_{rem}. The deflection of a rigid connected brace w_{fixed}, is calculated according to formula 2.15.

$$w_{fixed} = \frac{PL^3}{3EI} \tag{2.15}$$

The remaining deflection of the brace can be used to calculate the rotational displacement of the brace in the joint zone according to formula 2.16.

$$\theta = tan^{-1}(\frac{w_{rem}}{l_1}) \tag{2.16}$$

Equation 2.17 is used to calculate the rotation based on the top displacement u_{top}, bottom displacement u_{bottom} and brace height h_1 in the finite element analyses.

$$\psi = \arctan(\frac{u_{top} - u_{bottom}}{h_1}) \tag{2.17}$$

2.5 Buckling

When a structural element is subjected to a gradually increasing load, the load may reach a critical value that suddenly changes a member's respond or shape. The buckled element may lead to total failure of the entire structure. If not, the buckled element will continue to carry the load by redistributing the load to other parts of the structure. As a result, stresses may end up located in elements of the structure that cannot carry the load.
For braces with large cross-sections compared to the chord face, the large loads at the brace end will transfer the load to the chord side walls through the corners. As a result, the side walls will begin to buckle. The buckling will begin to stress the side wall, which makes it possible for the side wall to yield. Trahair 1993.

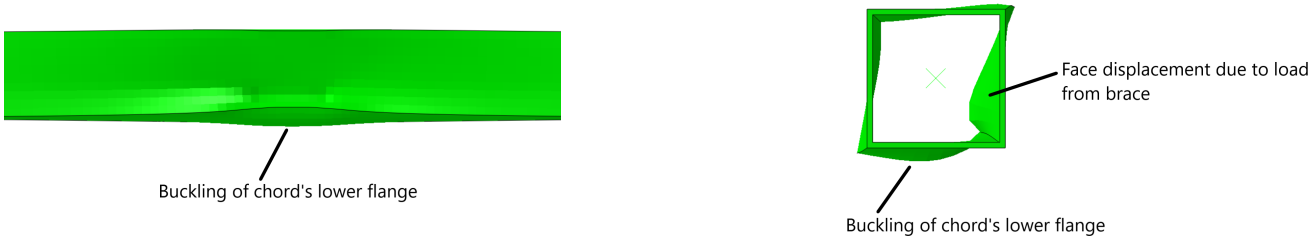

(a) (b)

Figure 2.2: Buckling of chords lower flange

2.6 Yield line theory

The yield line theory is based on the ultimate bending moment of a structural element at its collapsed state. It is an analysing method which uses a constant yield moment along a plate. When the structure is loaded, the steel is approaching the yielding stress. The areas where the yielding stress occurs follow straight lines from the point of loading to supporting edges. The first sign of yielding will occur along the yield lines. Bakker 1990.
Yield lines are straight, and by assuming their lengths and angles, it is possible to calculate the rotation of the structural element. The method of virtual work implies that by comparing the internal work W_i with the external work W_y, the ultimate bending moment can be calculated. See equation 2.18. Figure 2.3 shows the yield lines for both centric and eccentric placement of the brace.

$$\Sigma W_i = \Sigma W_y \tag{2.18}$$

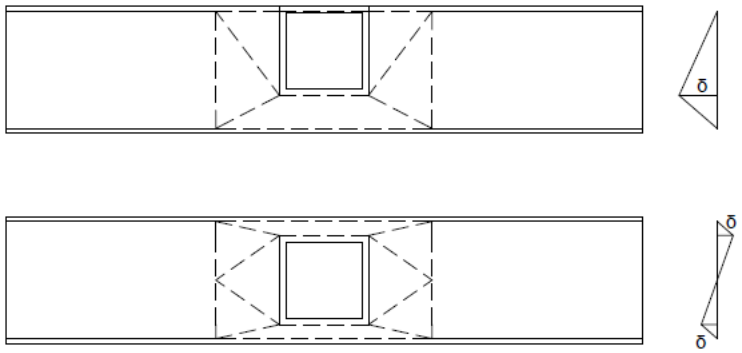

Figure 2.3: Possible yield line patterns for centric and eccentric placement of brace onto chord with rotation of the chord, inspired by Zhao et al. 2020

3 Finite element analysis

Finite element softwares are used to investigate the behaviour of eccentrically placed braces on chords. Softwares uses the finite element method described in section 3.1 to calculate displacement based on boundary conditions and loads applied. To perform the numerical study needed in this thesis, Abaqus will be utilized.

3.1 Finite element method

The goal of static stress analyses is typically to calculate the stresses, displacements, and strains within a geometric body. Internal stresses develop within a body in such a way as to maintain equilibrium over any volume of the body. Hence, equilibrium can be used to calculate stresses, displacements and strains over the entire body. It is easy to do for one-dimensional bodies but becomes harder for two-dimensional and three-dimensional bodies. The finite element method solves such problems by splitting the body into many small elements connected by nodes, called discretisation. Discretisation is helpful because the equilibrium requirement now only needs to be satisfied over a finite number of discrete elements instead of continuously over the entire body.
The essential variable to calculate when performing static stress analyses is the displacement of the nodes. It is easy to calculate both stresses and strains if the displacements are known. For each element, a vector $\{U\}$ can be defined which contains all possible displacements of the nodes of the element, including rotation. The number of possible displacements is called degrees of freedom. The finite element method can be simplified by thinking that the elements have a certain stiffness that resists rotation. The stiffness of elements is combined to a global stiffness matrix $[K]$, based on how to model is tied together. Continuity implies that elements connected to the same node will have the same displacements. The global stiffness matrix defines how the entire structure will displace under loading. The global stiffness matrix is a square matrix, which means that the number of rows and columns equals the number of degrees of freedom. In many structures, the elements can be aligned with different coordinate systems. Hence the stiffness matrix for each element has to be transformed to align with the global coordinate system. It can be done by multiplying the element stiffness matrix by a rotation matrix $\{R\}$. When the global stiffness matrix is calculated and transformed to align with the correct coordinate system, equation 3.1 can be solved to find the displacements $\{U\}$. To solve the equation, boundary conditions need to be specified. Boundary conditions are known displacements at certain nodes, typically because some are fixed. $\{F\}$ is the force vector, containing reaction forces at the supports and external forces which is applied to the structure. Dhatt et al. 2012.

$$\{F\} = [K]\{U\} \tag{3.1}$$

The equation can be solved by inverting the matrix to get $\{U\}$ by itself, but this is hard since the global stiffness matrix is sparse, meaning most of the elements in

the matrix is zero. The most common way of solving equations like this is by iterative approximating the displacement vector. The conjugate gradient method is a popular iterative method often used in equations like this. When the displacements are solved, using formula 2.2 and formula 2.3 are used to calculate the stresses and strains in the elements. A finite element mesh can easily contain hundreds of thousands of degrees of freedom, which is impossible to calculate by hand. This means that having anything other than a very basic model requires the use of appropriate softwares, like Abaqus.

3.2 Abaqus/Explicit

Abaqus has two main ways two calculate the results, Abaqus/Standard and Abaqus/Explicit. What method to be used depends on the problem. While Abaqus/Standard is more efficient at solving smooth nonlinear problems, Abaqus explicit is better suited for high-speed dynamic analyses. Abaqus/Standard can solve many problems but may have problems if there are material complexities. For example, large deformations or complex contact conditions may cause Abaqus/Standard difficulties converging due to many iterations. In those cases, Abaqus/Explicit is the best option.

3.3 Technical terms

In this subsection, some of the technical terms which is used in this thesis is explained.

Mesh

When using the finite element method explained in section 3.1, the body of a structural component is split into a finite number of elements and nodes. The collection of those elements and nodes is called the mesh. Creating a mesh on a structural component when using softwares can be done in multiple ways. The most popular way is by choosing a size for the elements. Abaqus then splits the component into elements of this size. One can also choose how many elements are wanted in the component. The size of the elements is then chosen to fit the number wanted.
The mesh on the component is of great importance. Finer mesh will have more exact stress and strain calculations, but the time for the analysis to finish increases. A coarser mesh will reduce the time for the analysis to run, but the results will be more inaccurate. Hence there is essential to choose a mesh that gives exact and representative results simultaneously as the analyses run at an acceptable time. In many cases, the mesh in the zone of interest is finer, like the joint zones. Zones which are not of interest will have a coarser mesh to reduce the run time for the analysis.

Solid elements

The mesh elements used in the models in this thesis are C3D8R solid elements. This element is an 8-node linear brick. The element is suited to perform linear and complex nonlinear analyses where contact and large deformations will be present.

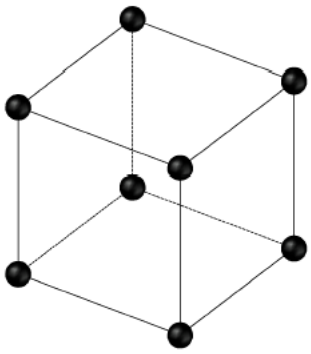

Figure 3.1: C3D8R Solid element with nodes in the corners

The elements are also well suited to perform stress analyses. The element has reduced integration, which means using a lower-order integration to form the element stiffness matrix. However, the mass matrix and distributed loadings are still made using full integration, SIMULIA 2011.

Tie-constraint

A tie constraint ties surfaces or nodes together, so there is no relative motion between them. This thesis uses surface to surface ties to mimic the welding between the brace and chord. A master and slave surface needs to be chosen to tie together surfaces. The master surface is typically the surface with the coarsest mesh. Since the mesh in the joint zone is the same in this thesis, it does not matter what surface chosen is to be master or slave. When two surfaces are chosen, the shortest distance between the surfaces is calculated and tied together. Hence, elements at the surfaces which has a longer distance to the other surface will have no ties, giving the surface the option to deform independently from the other surface.

Rigid body constraint

A rigid body constraint means that one can constrain the motion of a region to the motion of a reference point. In this thesis, the motion of the chord ends is constrained to the motion of reference points placed at the chord ends. The constraint makes it possible to change the boundary conditions at the chord ends quicker.
When defining a rigid body constraint, choosing from multiple different ways of constraining the region is possible. In this thesis, the chord ends are pinned to the motion of the reference points, meaning translational and rotational displacements are constrained to the motion of the reference point.

Coupling constraint

Coupling constraint constrains the motion of a node region to the translational and rotational motion of a reference point. Loads or boundary conditions can then be applied to the reference point. The reference point distributes the load to the surface nodes by weight factors. In this thesis, coupling constraints are used at the brace end to distribute the loads over the entire cross-section of the brace. The coupling here has only the rotational motion of the surface constrained to the reference point.

3.4 Modelling procedure

A larger portion of this thesis is modelling parts where the brace is placed centric and eccentrically onto the chord, with changing β-values. Abaqus is a finite element analysis solver which can be used to model three-dimensional instances to investigate how certain loads affect the modelled instance. Section 3.4.1 to 3.4.6 explains how to model is made and ran in Abaqus.

3.4.1 Part

The model is made of two parts, a chord and a brace. Both those parts were drawn using solid extrusion by drawing the cross-section of the brace and then extruding the cross-section in the longitudinal direction. Table 2 presents the geometric data for the chord and brace, which is modelled for the primary investigation. The length of the parts depends on the cross-sections of the parts. According to Zhao et al. 2020, the length of the chord must be $L_{chord} = 10h_0$ and the brace length must be $L_{brace} = 8h_1 + b_0$ to reduce the effects of the boundary conditions from the ends in the joint-zone. The cross-sections are gathered from Larsen et al. 2003

Chord	Brace	$L_{Chord}(mm)$	$L_{Brace}(mm)$	$\beta(-)$
200×200 × 8	100×100 × 10	2000	1000	0.50
200×200 × 8	120×120 × 10	2000	1160	0.60
200×200 × 8	140×140 × 10	2000	1320	0.70
200×200 × 8	160×160 × 10	2000	1480	0.80
200×200 × 8	170×170 × 10	2000	1560	0.85
200×200 × 8	180×180 × 10	2000	1640	0.90
200×200 × 8	190×190 × 10	2000	1720	0.95

Table 2: Geometric data for chord and brace used in the main models

3.4.2 Material

The material assumed in the analyses is S355 steel. Typical material properties are presented in table 1, stresses and strains used to create the material behaviour is presented in table 3.

	Stress (N/mm^2)	Strain (-)
Elastic	355	0
Plastic	470	0.178

Table 3: Stress-strain limits used in FEA.

3.4.3 Step

Creating the step defines how the load is applied to the instance. For the models used in this investigation, the step is created as a general static step. Meaning the

loads are applied over a set time. Due to the importance of recognizing the step where the stresses in the elements reach 470 Mpa, the increments are small. Smaller increments secure smoother load application, making it easier to recognize the step where the stress reaches the ultimate stress. The increment sizes is presented in table 4.

Initial	Minimum	Maximum
0.002	10^{-15}	0.01

Table 4: Increment sizes used in the analyses

3.4.4 Interaction

The interaction step provides information about how the parts react to collision with other parts and how the parts are attached using constraints. Frictional contact and 'hard' contact is used between the brace and chord. Three different constraints were utilized to attach the model. Due to simplicity, a tie constraint was used to simulate the weld between the chord and brace. The chord's face is used as the master surface, while the brace's cross-section is used as the slave. See figure 3.2a. At the chord ends, rigid body constraints are used to tie the ends to reference points for faster marking of the chord cross-section. The cross-section of the chord is pinned to the reference points at the ends. See figure 3.2b. The brace end is tied to a reference point with a continuum distributing coupling constraint. This constraint only has translational degrees of freedom coupled in (U1, U2, U3). See figure 3.2c.

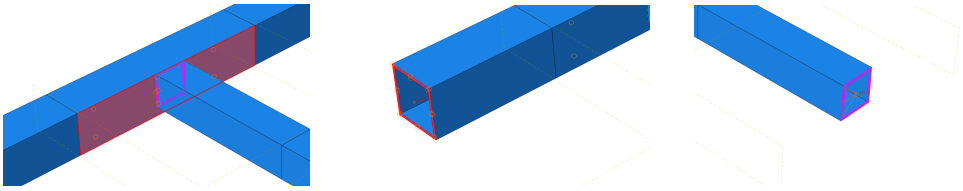

(a) Tie constraint (b) Rigid body constraint (c) Coupling constraint

Figure 3.2: Comparison between different constraints used in the models

3.4.5 Loads

Applying loads to the instance means defining loads and boundary conditions to the structure. The chord ends are encastred, which means that translational and rotational displacements are constrained. See figure 3.3a. There is also a load placed at the end of the brace. The brace end load is defined as a displacement. This displacement moves the brace end downwards to the point where an element in the chord reaches the ultimate stress. A table with forces can then be extracted where there is a force corresponding with displacements and stresses throughout the analysis. See figure 3.3b.

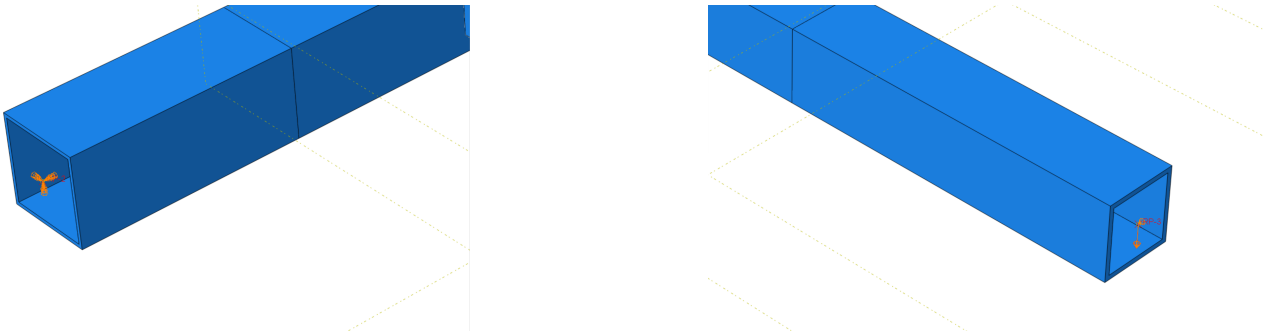

(a) Encastred chord ends (b) Displacement load at brace end

Figure 3.3: Boundary conditions and loads applied to the instance

3.4.6 Mesh

Initially, partitions on the chord and brace were created on the parts. Two partitions split the chord into three pieces, while a partition split the brace in half. Because of those partitions, it is possible to have different mesh over the length of the parts. The joint zone had finer mesh, while the chord and brace's end parts had coarser mesh. As mentioned in section 3.3, finer mesh gives more exact results but increases the run time. The end regions of the parts had coarser mesh since these areas were less critical. Hence it is possible to reduce the run time of the analyses.

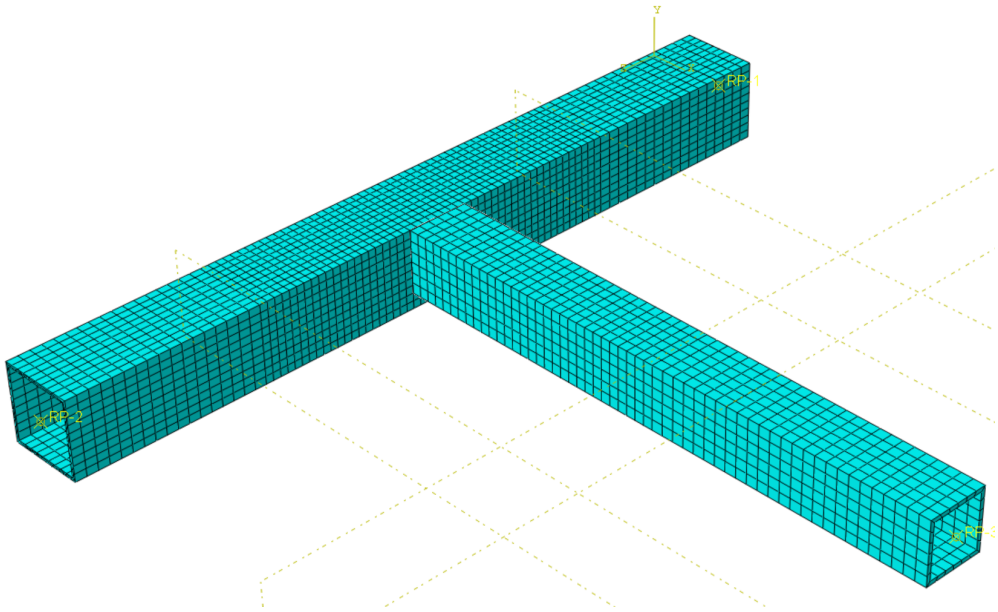

Figure 3.4: Meshing of the instance

3.4.7 Post processing of results

After the analyses have been run, forces and displacement of the chord face are saved. The last force to be exported is the force in which a node at the chord reaches the ultimate stress. It represents the maximum force the instance can take

before failure. The results are then transferred to a MatLab script which analyses the data. The code calculates the moments based on the force input, while the displacements of the chord face are used to calculate the rotational displacement of the chord face. At this point, the MatLab code plots the moment-rotation curve. Capacity losses for elastic and plastic capacity are calculated and plotted to investigate how the capacity loss develops.

4 Experimental test

4.1 Introduction

Based on the available literature on this subject, there is only one test like this performed earlier. The test performed had some differences in the cross-sections and made use of a steel plate to attach the top flange of the braces. A small test on a T-joint with out-of-plane bending moment was then performed.

4.2 Setup

The cross-section of the chord was made of a $80 \times 80 \times 4$ RHS profile, while the chord was made of a $50 \times 50 \times 5$ RHS profile. Those cross-sections makes β=0.625. The brace was welded to the chord using fillet welds around the brace's lower flange and side walls, while the top flange of the brace was attached to the chord using a flare bevel weld. See figure 4.1. The entire instance was then fastened to a wall using

Figure 4.1: Welds between brace and chord, a=3mm

flat steel plates. At the backside of the chord, 5mm thick flat steel plates were used to created distance between the structure and wall. Four nuts were used to tighten the chord so that it could not move during loading. The distance between the bolt fasteners were 500mm. The instance is loaded using dead-wights placed at a loading plate attached to the brace end. The loading plate was stopped from gliding off the brace due to a stopper at the brace end. See figure 4.2.

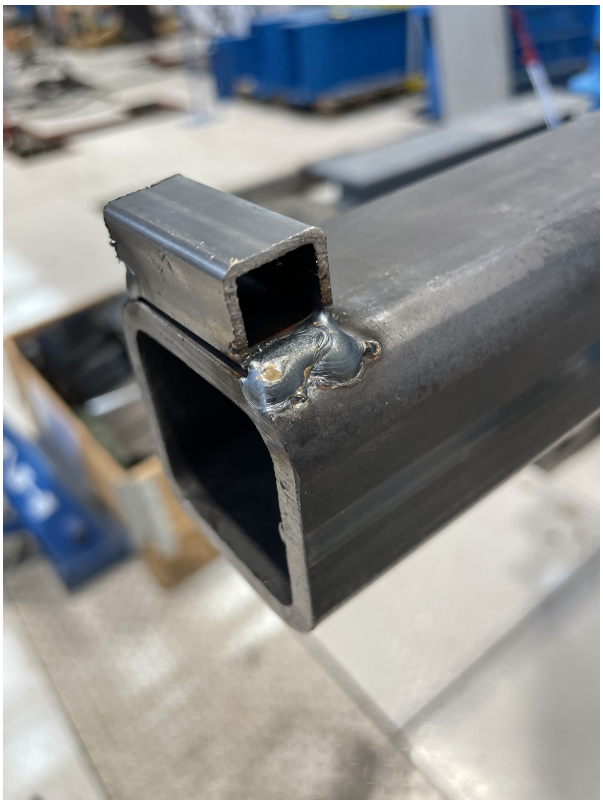

Figure 4.2: Stopper at brace end

Displacement sensors were also placed at the chord face and chord top flange to monitor the displacements during loading. The entirety of the instance can be seen in figure 4.3.

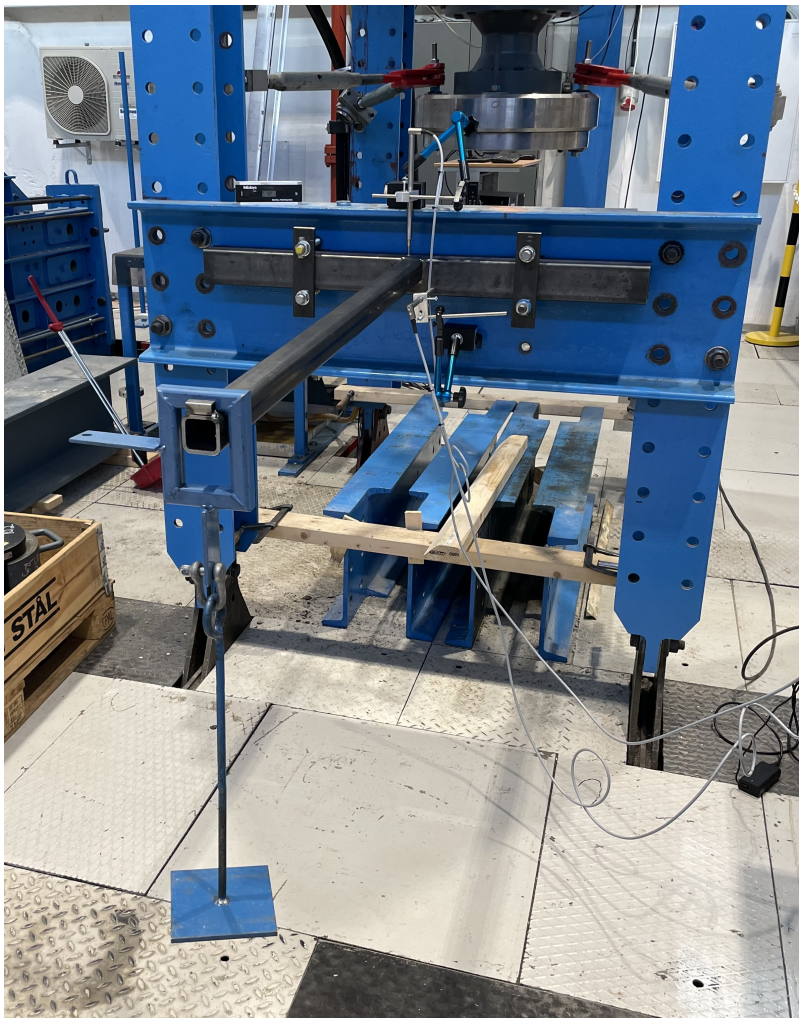

Figure 4.3: Experimental setup

4.3 Procedure

Firstly, the rotational displacement of the brace was measured to find out how much the brace was displacing due to self-weight. The vertical distance from the loading plate to the floor was also measured. Afterwards, dead loads were placed at the loading plate at the end of the brace. After increasing the load, a new rotational measurement of the brace was made, and displacements at the chord face and top flange were noted. The vertical deflections were also monitored.

4.4 Finite element analysis

The finite element model was mostly made according to section 3.4, but some geometrical changes had to be made to make the model represent the physical instance. The geometrical data, which was measured from the physical instance and used to make the finite element model, can be seen in table 5.
The model was then displaced with the maximum deflection measured. The results from the finite element analysis can be seen in figure 4.5.

	Chord	Brace
l (mm)	1000	1140
h (mm)	80	50
b (mm)	80	50
t (mm)	4	5

Table 5: Geometrical data to create the finite element model

4.5 Results and comparison

The rotational displacement of the chord face is calculated as explained in section 2.4. The results are presented in table 6.

Load (kg)	$w_{tot}(mm)$	$w_{fixed}(mm)$	$w_{rem}(mm)$	$\theta_{cal}(rad)$	$\theta_{meas}(rad)$
4	0	0	0	0	0
24	19	1.87	17.13	0.015	0.014
74	34	5.77	28.23	0.025	0.031
124	57	9.66	47.34	0.041	0.045
144	77	11.22	65.78	0.058	0.07
164	107	12.78	94.22	0.082	0.087
174	128	13.56	114.44	0.1	0.105
184	148	14.34	169.66	0.117	0.126
194	172	15.12	156.88	0.137	0.14
204	188	15.9	172.1	0.15	0.157
214	206	16.68	189.32	0.165	0.171
224	224	17.46	206.54	0.179	0.197
234	242	18.24	223.76	0.194	0.2
244	256	19.02	236.98	0.205	0.22
264	277	20.58	256.42	0.221	0.233
274	295	21.36	274.64	0.236	0.243
284	312	22.13	289.87	0.249	0.251
294	326	22.91	303.09	0.26	0.297

Table 6: Calculated deflections and rotations compared to measured rotation

The deformation of the chord face can be seen in figure 4.4, where also the yield line pattern described in section 2.6 can be seen. The results from the experiment and the finite element analysis can be seen in figure 4.5.

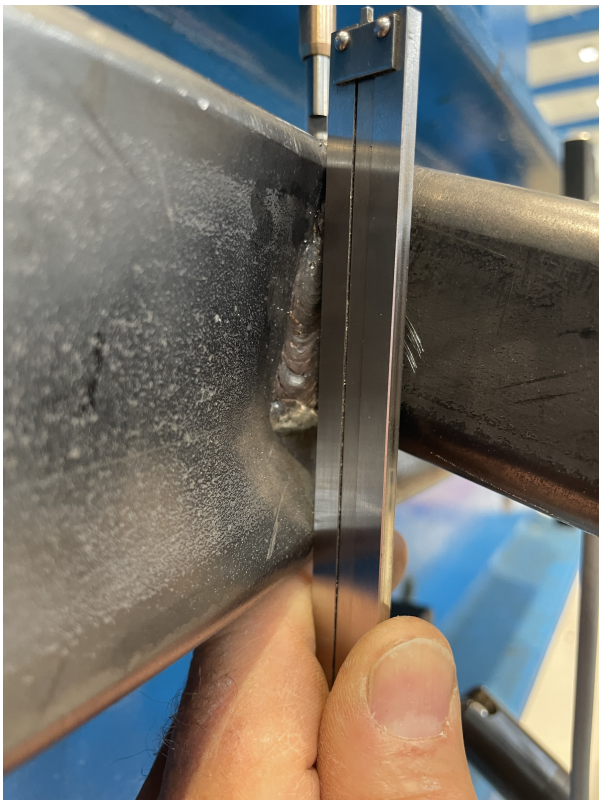

Figure 4.4: Deformation of chord face after loading

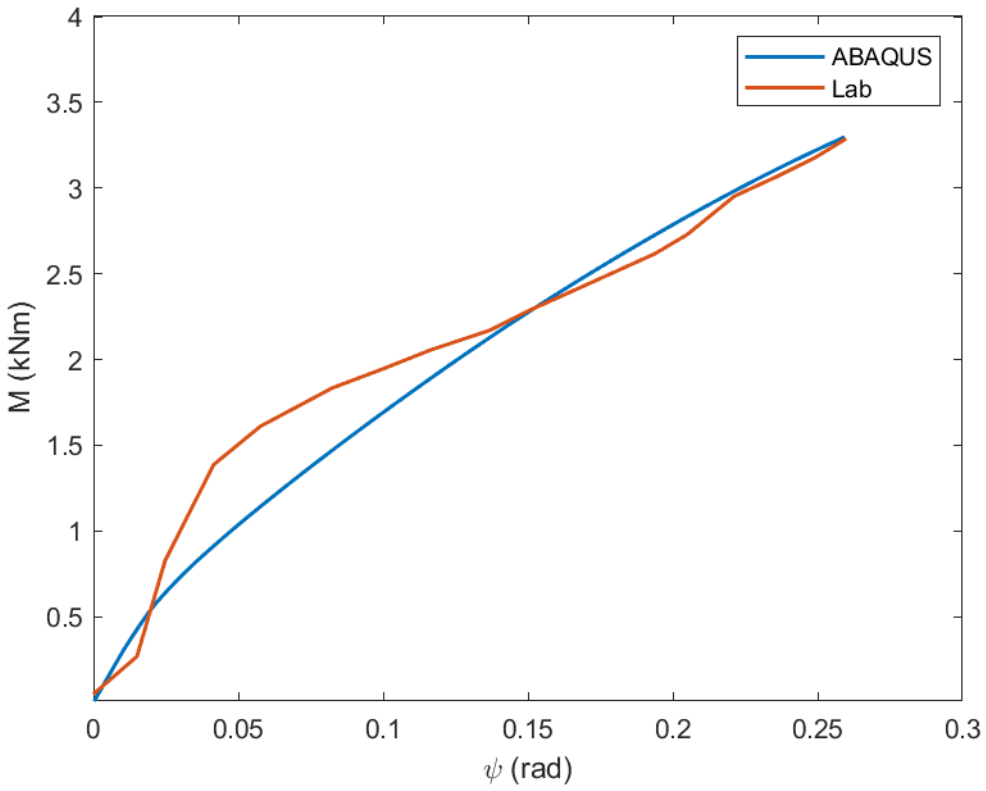

Figure 4.5: Moment-rotation curve from experiment compared to finite element analysis

4.6 Discussion

The instance used in the experimental test had many sources which could influence the results. The loading frame which was sat at the brace end was not fastened. It was just placed on the brace and stopped from gliding off by the stopper at the brace end. Since the clamp was not fastened properly, the clamp could tilt, making the load more dominant on one side of the brace. The clamp could have made a torsional buckling effect on the brace, making the forces transferred to the chord skewed.

The brace was fastened to the wall using flat steel plates. Because the steel plates were squeezing the chord face, some rotational displacement could have been detained. A better solution is to weld the chord ends to plates.

The weights planted at the loading plate reached the top of the loading plate during the loading, making it hard to put on any more weight. Some of the weights that had already been planted had to be removed to replace them with heavier weights. The de-loading of the loading plate made the instance relapse and harden due to "cyclic" loading. The "cyclic" loading may have influenced the behaviour of the joint zone.

Some of the weights were also very hard to hold on to, making it hard to place the weights onto the loading plated steadily. The sudden weight drop onto the loading plate made the brace swing a small amount. The swinging of the brace could rotate the face of the chord more than it would have if the weights were dropped more steadily.

5 Analysis results

The following subsections presents the results from the 14 finite element analyses which were ran. The sections also contains comparison between the centric and eccentric models. Explanations and discussions are presented in section 6.

5.1 Results for RHS 100 × 100

The cross-sectional data used in the making the model with β=0.50 is presented in table 7.

Profile	h $\times b \times t(mm)$	Length(mm)	Part
RHS 200×200	200×200 × 8	2000	Chord
RHS 100×100	100×100 × 10	1000	Brace

Table 7: Geometric data for brace and chord with β=0.50

Two models were created to investigate the behaviour of centric and eccentric placement of the brace onto the chord. Figure 5.1a and figure 5.1b shows the difference between the two models used in the investigation.

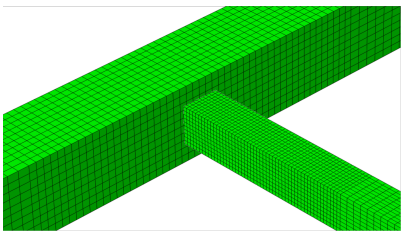

(a) Centric placement of brace

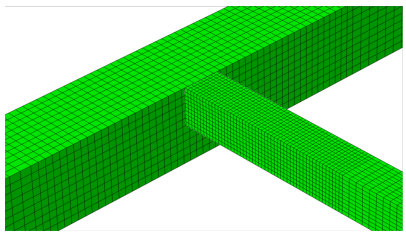

(b) Eccentric placement of brace

Figure 5.1: Placements of brace used in the models with β=0.50

The results from the analyses can be seen in figure 5.2 and table 8.

β=0.50	Centric (kNm)	Eccentric (kNm)	Capacity loss (%)
Elastic capacity	10,6	3,1	71
Plastic capacity	79,6	46,4	42
EC3 capacity	11,3	-	-

Table 8: Capacity comparisons between centric and eccentric model

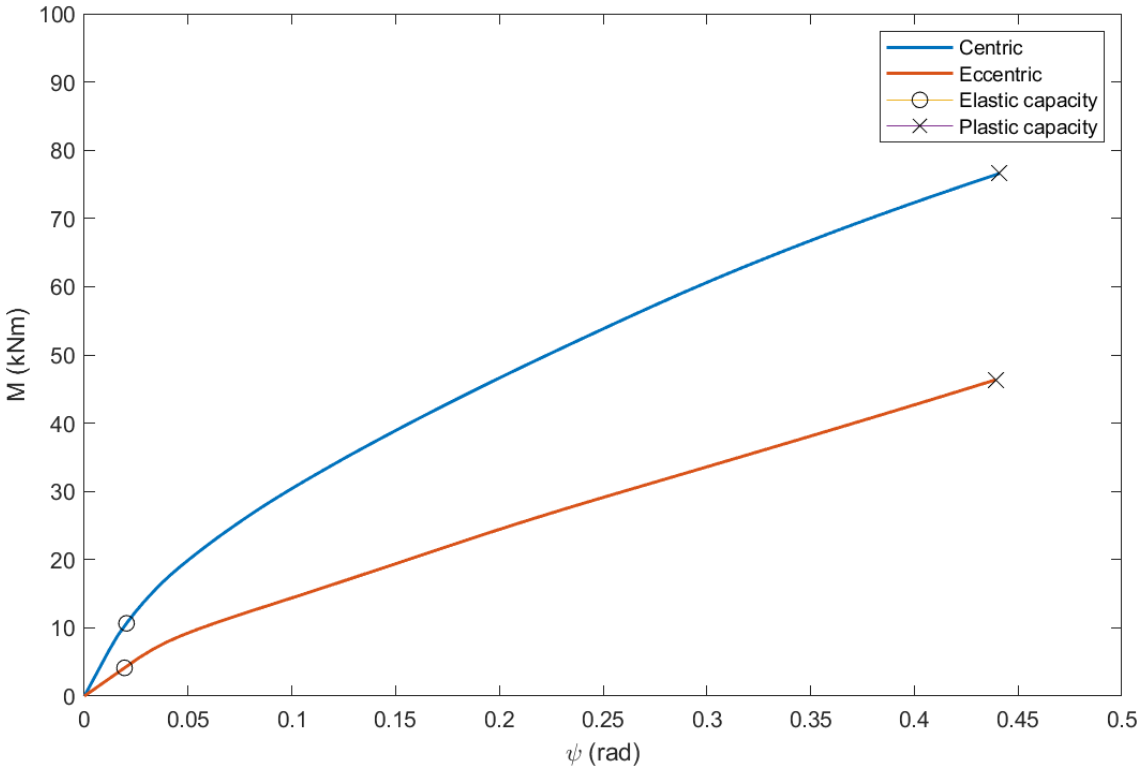

Figure 5.2: Moment-rotaion curves for β=0.50

5.2 Results for RHS 120 × 120

The cross-sections used in the making of the model with β=0.60 is shown in table 9.

Profile	h $\times b \times t(mm)$	Length(mm)	Part
RHS 200×200	200×200 × 8	2000	Chord
RHS 120×120	120×120 × 10	1160	Brace

Table 9: Geometric data for brace and chord with β=0.60

The two models used to investigate the behaviour of centric and eccentric placement of the brace onto the chord is shown in figure 5.3a and figure 5.3b.

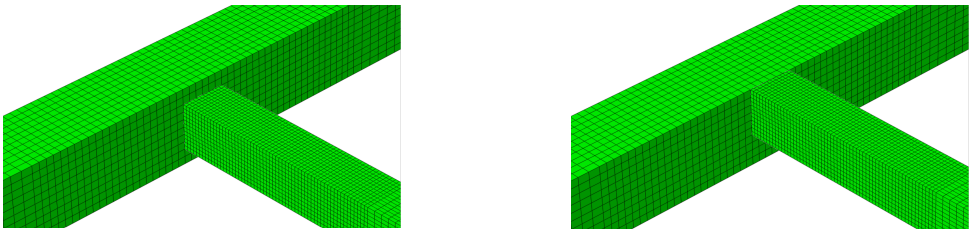

(a) Centric placement of brace (b) Eccentric placement of brace

Figure 5.3: Placements of brace used in the models with β=0.60

The results from the analyses can be seen in figure 5.4 and table 10.

β=0.60	Centric (kNm)	Eccentric (kNm)	Capacity loss (%)
Elastic capacity	13,2	5,9	55,3
Plastic capacity	74,5	59,0	21
EC3 capacity	15,4	-	-

Table 10: Capacity comparisons between centric and eccentric model

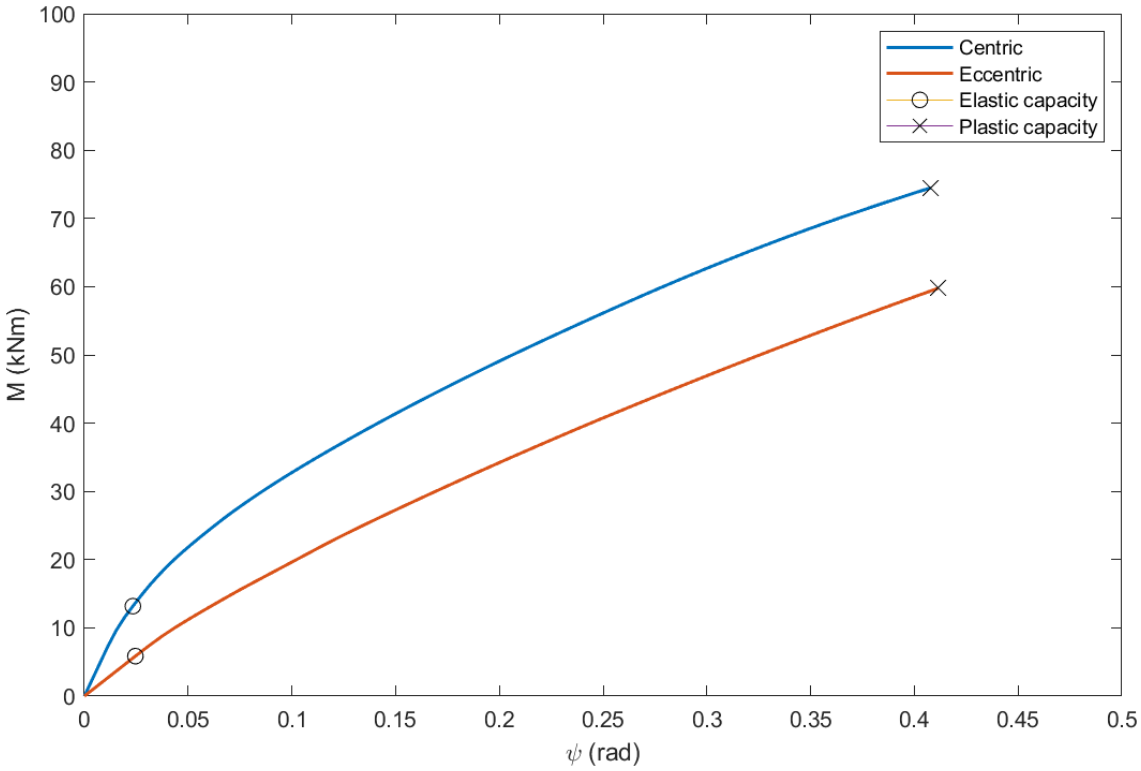

Figure 5.4: Moment-rotaion curves for β=0.60

5.3 Results for RHS 140 × 140

Table 11 shows the cross-sectional data used in the FEA-analysis with β=0.70. The two variants of the model with β=0.70 can be seen in figure 5.5a and figure 5.5b.

Profile	h $\times b \times t(mm)$	Length(mm)	Part
RHS 200×200	200×200 × 8	2000	Chord
RHS 140×140	140×140 × 10	1320	Brace

Table 11: Geometric data for brace and chord with β=0.70

The results from the analyses can be seen in figure 5.6 and table 12.

	Centric (kNm)	Eccentric (kNm)	Capacity loss (%)
Elastic capacity	22,9	8,2	64,2
Plastic capacity	107,2	76,4	29
EC3 capacity	21,8	-	-

Table 12: Capacity comparisons between centric and eccentric model

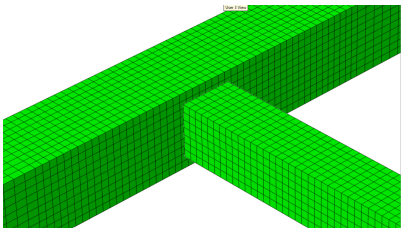

(a) Centric placement of brace

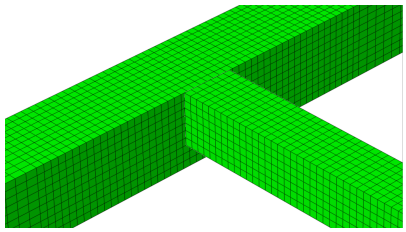

(b) Eccentric placement of brace

Figure 5.5: Placements of brace used in the models with β=0.70

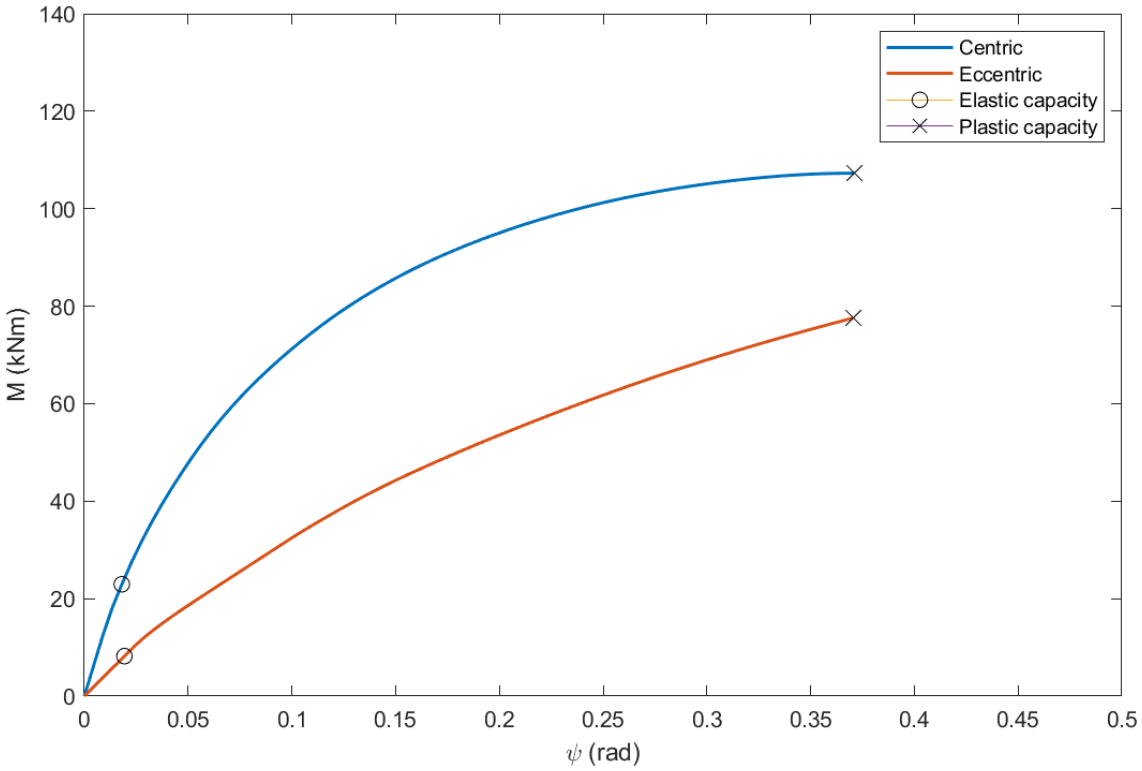

Figure 5.6: Moment-rotaion curves for β=0.70

5.4 Results for RHS 160 × 160

The cross-sectional data used in the FEA-analysis can be seen in table 13. The two variants of the model can be seen in figure 5.7a and figure 5.7b.

Profile	h $\times b \times t(mm)$	Length(mm)	Part
RHS 200×200	200×200 × 8	2000	Chord
RHS 160×160	160×160 × 10	1480	Brace

Table 13: Geometric data for brace and chord with β=0.80

The results from the analyses can be seen in figure 5.8 and table 14.

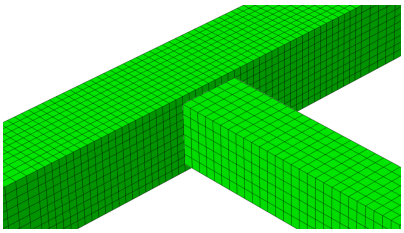

(a) Centric placement of brace

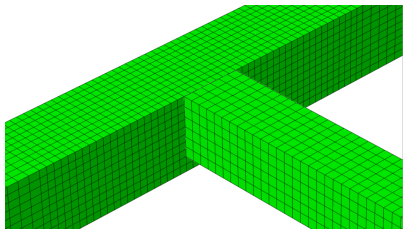

(b) Eccentric placement of brace

Figure 5.7: Placements of brace used in the models with β=0.80

β=0.80	Centric (kNm)	Eccentric (kNm)	Capacity loss (%)
Elastic capacity	34,2	25,3	26
Plastic capacity	108,7	94,0	14
EC3 capacity	33,6	-	-

Table 14: Capacity comparisons between centric and eccentric model

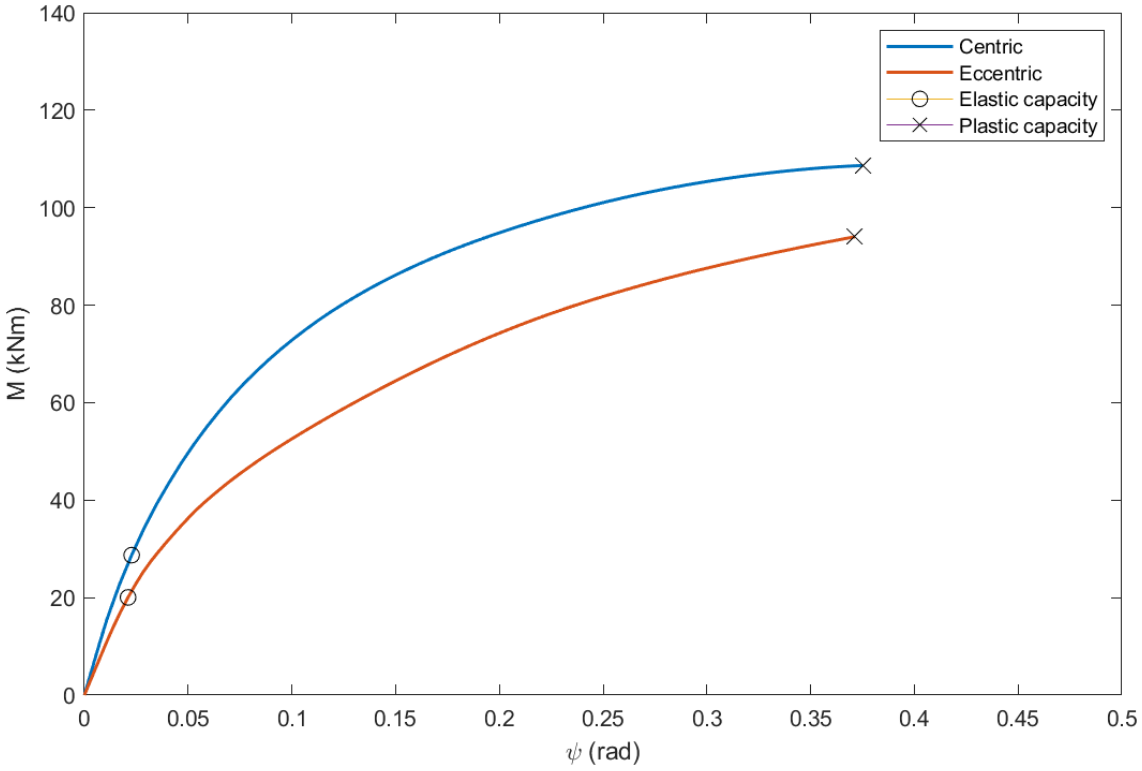

Figure 5.8: Moment-rotaion curves for β=0.80

5.5 Results for RHS 170 × 170

Table 15 presents the cross-sectional data used to model brace and chord with β=0.85. Figure 5.9a and figure 5.9b shows the two variants used to investigate the behaviour of centric and eccentric placement of the brace.

The results from the analyses can be seen in figure 5.10 and table 16.

Profile	h $\times b \times t(mm)$	Length(mm)	Part
RHS 200×200	200×200 × 8	2000	Chord
RHS 170×170	170×170 × 10	1560	Brace

Table 15: Geometric data for brace and chord with β=0.85

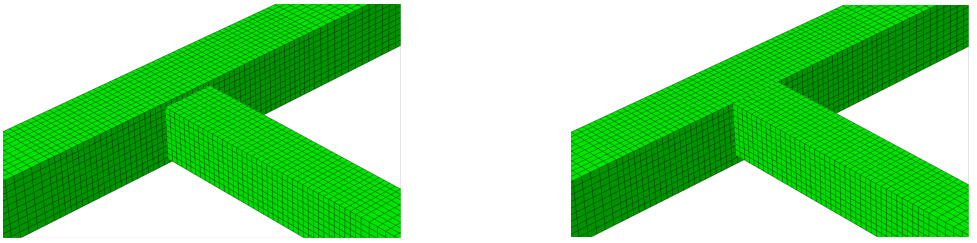

(a) Centric placement of brace (b) Eccentric placement of brace

Figure 5.9: Placements of brace used in the models with β=0.85

β=0.85	Centric (kNm)	Eccentric (kNm)	Capacity loss (%)
Elastic capacity	44,5	35,3	21
Plastic capacity	125,5	114,9	8
EC3 capacity	44,6	-	-

Table 16: Capacity comparisons between centric and eccentric model

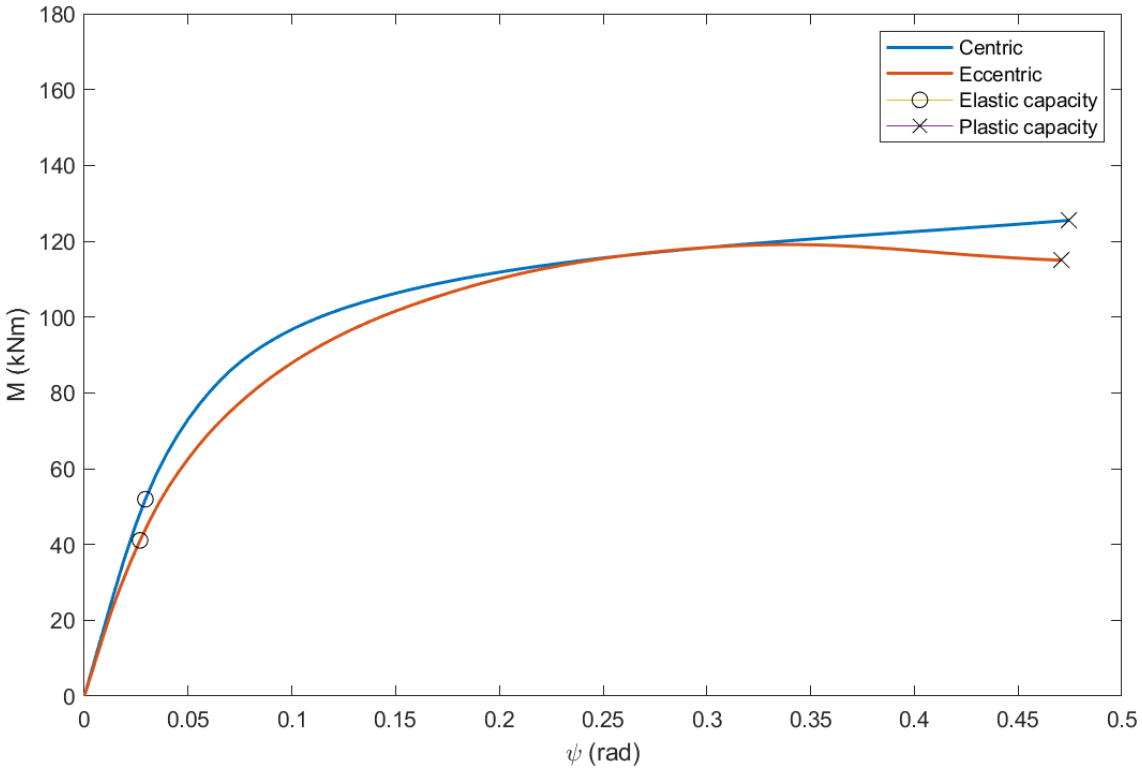

Figure 5.10: Moment-rotaion curves for β=0.85

5.6 Results for RHS 180 × 180

Table 17 shows the cross-sectional data used for chord and brace, wile figure 5.11a and figure 5.11b shows the two variants of the model.

Profile	h $\times b \times t(mm)$	Length(mm)	Part
RHS 200×200	200×200 × 8	2000	Chord
RHS 180×180	180×180 × 10	1640	Brace

Table 17: Geometric data for brace and chord with β=0.90

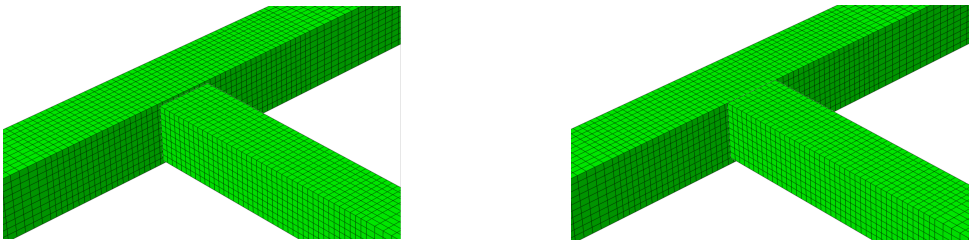

(a) Centric placement of brace (b) Eccentric placement of brace

Figure 5.11: Placements of brace used in the models with β=0.90

The results from the analyses can be seen in figure 5.12 and table 18.

β=0.90	Centric (kNm)	Eccentric (kNm)	Capacity loss (%)
Elastic capacity	65,5	50,7	23
Plastic capacity	127,8	111,7	13
EC3 capacity	65,4	-	-

Table 18: Capacity comparisons between centric and eccentric model

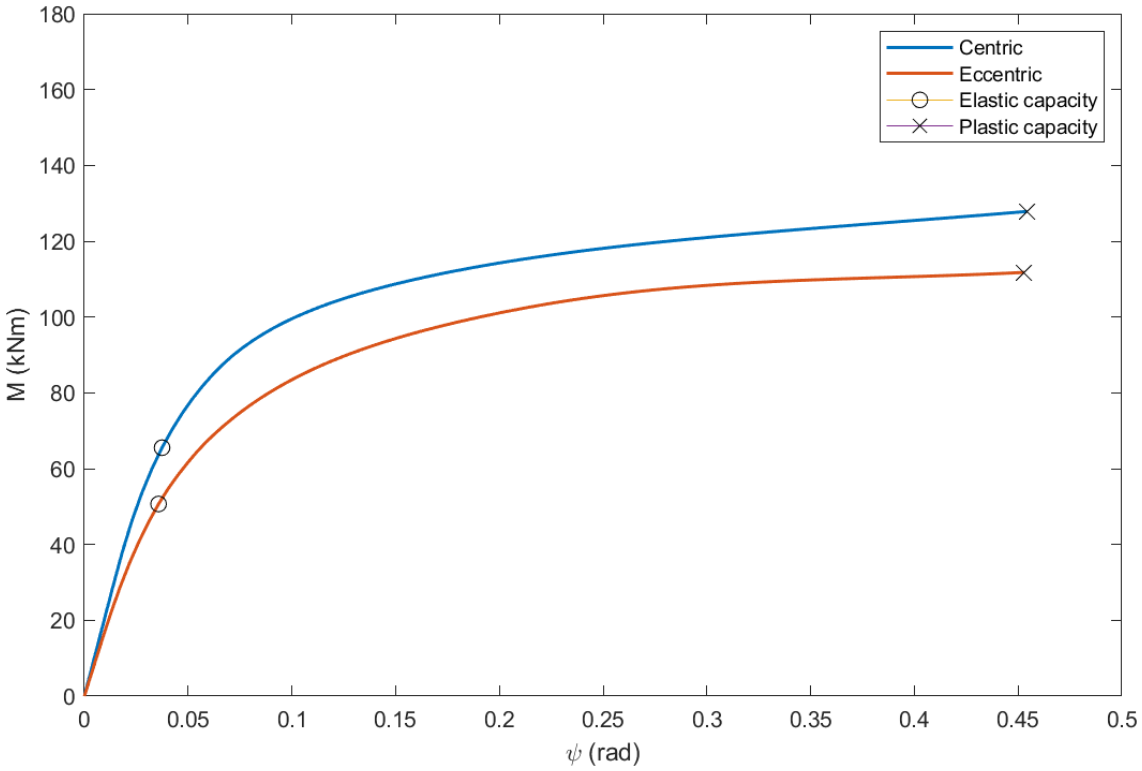

Figure 5.12: Moment-rotaion curves for β=0.90

5.7 Results for RHS 190 × 190

The cross-sections used to make the model can be seen in table 20, while figure 5.13a and figure 5.13b shows the two variants of the model investigated.

Profile	h $\times b \times t(mm)$	Length(mm)	Part
RHS 200×200	200×200 × 8	2000	Chord
RHS 190×190	190×190 × 10	1720	Brace

Table 19: Geometric data for brace and chord with β=0.95

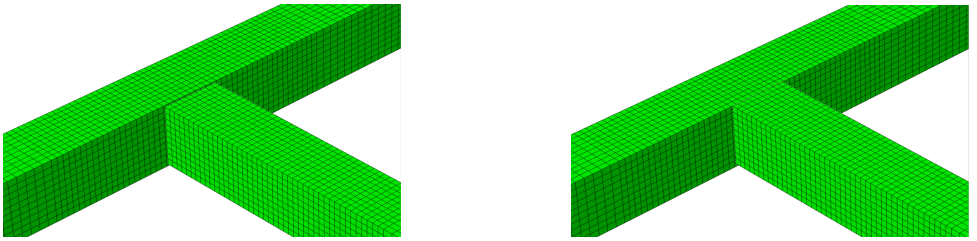

(a) Centric placement of brace (b) Eccentric placement of brace

Figure 5.13: Placements of brace used in the models with β=0.95

The results from the analyses can be seen in figure 5.14 and table 20.

β=0.95	Centric (kNm)	Eccentric (kNm)	Capacity loss (%)
Elastic capacity	70,2	70,0	<1
Plastic capacity	130,2	129,8	<1
EC3	72,8	-	-

Table 20: Capacity comparisons between centric and eccentric model

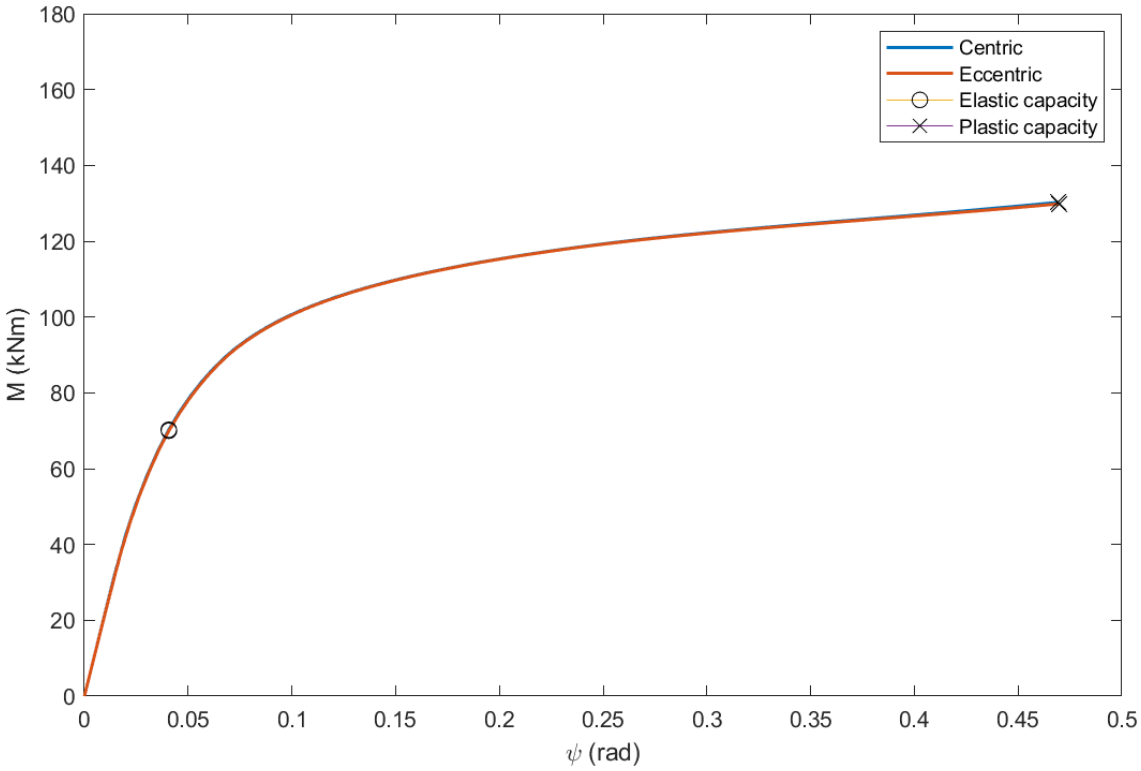

Figure 5.14: Moment-rotaion curves for β=0.95

6 Discussion

6.1 Analysis results

6.1.1 Results for RHS 100 × 100

As figure 5.2 shows, both the centric and eccentric model contains a linear part at the beginning of the curves. The linear part represents the moment-rotation behaviour of the instance before reaching the yield stress. The instance has the highest resistance against rotation of the chord face at this stage, which can be seen by the steep climb of the curve.
When the stress has reached the yield stress, the instance enters the plastic area. Deformations at this state are irreversible. Due to the rotational displacement of the chord face made in the elastic area, the instance becomes less stiff. Due to the loss of stiffness, the chord face will rotate more when the load increases. The loss of stiffness makes the curves have a slacker climb in the plastic area.

6.1.2 Results for RHS 120 × 120

The results from the analyses where β=0.60 can be seen in figure 5.4. The results can be seen to have a linear part representing the elastic region of the material at the beginning of the curves.
The part of the curve representing the plastic area of the instance has a steeper climb than for β=0.50. As mentioned earlier, increasing the cross-section of the instance makes it stiffer. The load has to be larger to rotate the face of the chord.

6.1.3 Results for RHS 140 × 140

Figure 5.6 shows the results form the analyses where β=0.70. As previous results have shown, there is initially a linear part representing the elastic region of the instance.
When entering the plastic region, it can be seen that the curve representing the centric model behaves differently than previous results. Since the distance from the brace lower flange is closer to the chord corners, they resist rotation of the chord's face more than previously. The resistance from the corners transfers the stresses to the side walls of the chord. When the load increases, the corners become deformed, thus not being able to resist the rotation of the chord face. Sudden failure then follows, making the chord face rotate much without an increased load.
For the eccentric model, the brace to corner distance is too large for the corners to resist rotation of the chord face. Hence, the curve representing the plastic region of the instance continuous following a linear path.

6.1.4 Results for RHS 160 × 160

Unlike previous results, the cross-section used when β=0.80 is large enough to chord face rotation resisted by the chord corners for both the centric and eccentric model. The resistance can be seen by the parabolic shape of the curves in figure 5.8.

6.1.5 Results for RHS 170 × 170

As seen in figure 5.10, the stiffness for the eccentric model begins to close up to the stiffness of the centric model. β=0.85 is an intricate value for this type of joint and loading. This value marks the cross-sectional differences which transfer the stresses to the chord side walls through the corners of the chord. Hence, the stresses in the chord side walls are close to the chosen limits. For the eccentric model, the distance from the lower brace flange to the chord corners is too large for the stresses to be as large in the side walls as the chord face.

6.1.6 Results for RHS 180 × 180

As figure 5.12 shows, the stiffness between the centric and eccentric models is almost the same due to the small distance the brace has to be moved to create the eccentric model from the centric model. As mentioned previously, the model is now inside the region where the side walls of the chord reach failure first. Failure of the side walls is the failure mode for the eccentric model too.

6.1.7 Results for RHS 190 × 190

Figure 5.14 shows the results from the analyses where β=0.95. The vertical distance between the brace in the centric and eccentric model is so small that there is no visible difference between the curves. As for β=0.90, the failure is located in the chord side walls.

6.2 Elastic capacity of joint

As expected, the elastic capacity of the eccentric placed brace members increases when the β-value increases. The increase in elastic capacity is due to a larger cross-section that can carry larger loads, and the corners of the chords face resisting rotation. As seen in figure 6.1, the elastic capacity of the models increases exponentially with increasing β. When β increases, the corners will resist rotation of the chord's face, making it possible for the brace to carry a larger load before it starts to displace the face of the chord. While the corners resist the displacement of the chord face, a larger portion of the stresses is transferred to the chord side wall, making it buckle.

6.3 Plastic capacity of joint

The plastic capacity of the instance increases with increasing β. The plastic capacity increase can also be explained by the cross-section of the brace increasing, being able to carry larger loads. The plastic capacity of the member increases approximately linearly. The exception is when β=0.85. The linear increase happens due to the deformation of the chord corners, which deforms linearly with increased load. When they are deformed, they can not resist rotational displacement of the chord face anymore, resulting in sudden failure of the chord face or side wall.

6.4 Capacity loss

When the cross-section of the brace is increased, the vertical distance which separates the centric and eccentric placement becomes smaller, resulting in the lower flange of the brace being put closer to the lower flange of the chord. The corners of the chord will then have a larger impact in resisting the rotational displacement of the

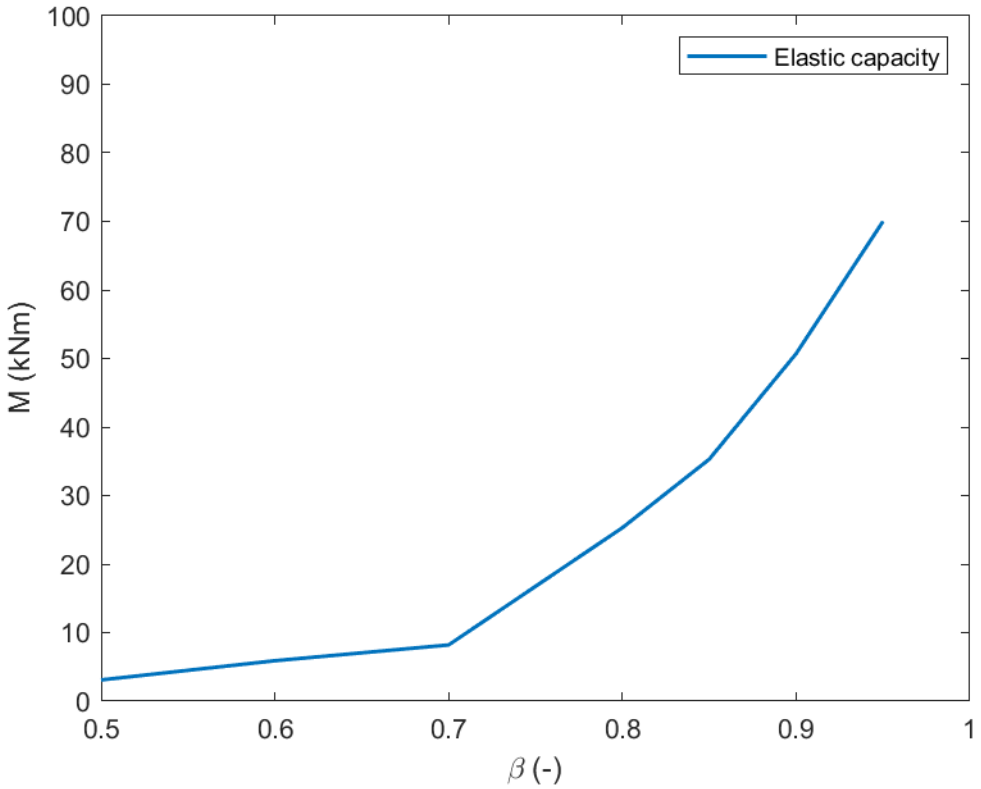

Figure 6.1: Development of elastic capacity

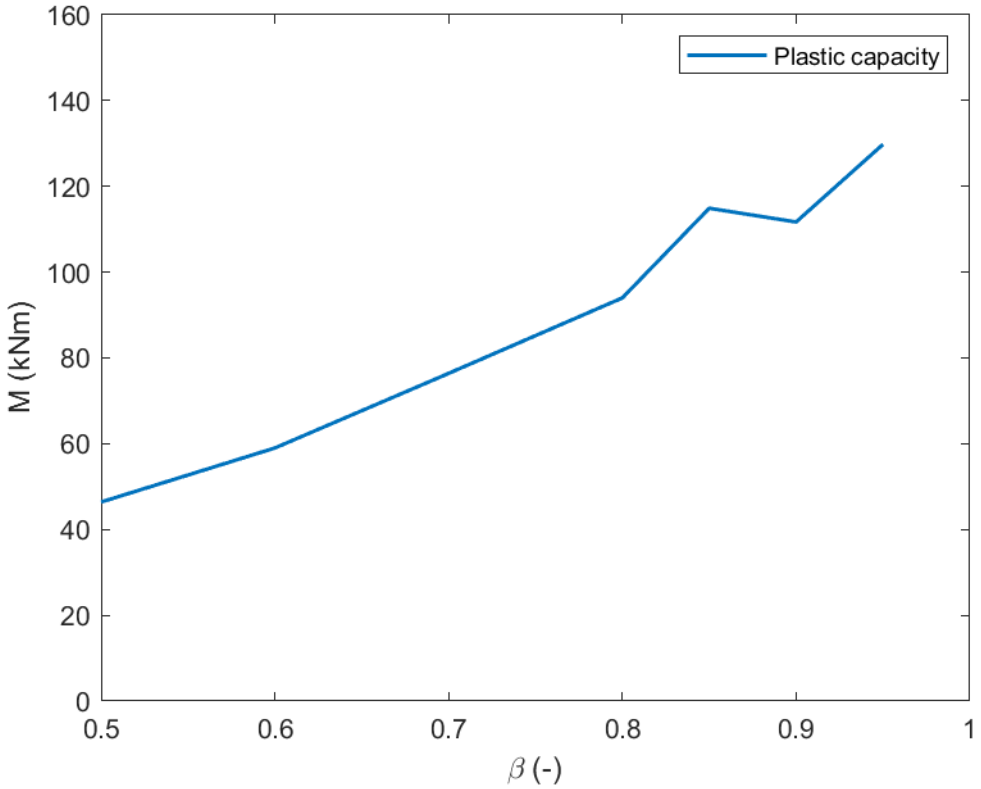

Figure 6.2: Development of plastic capacity

chord face. The eccentric model will then be able to carry larger loads before failure.

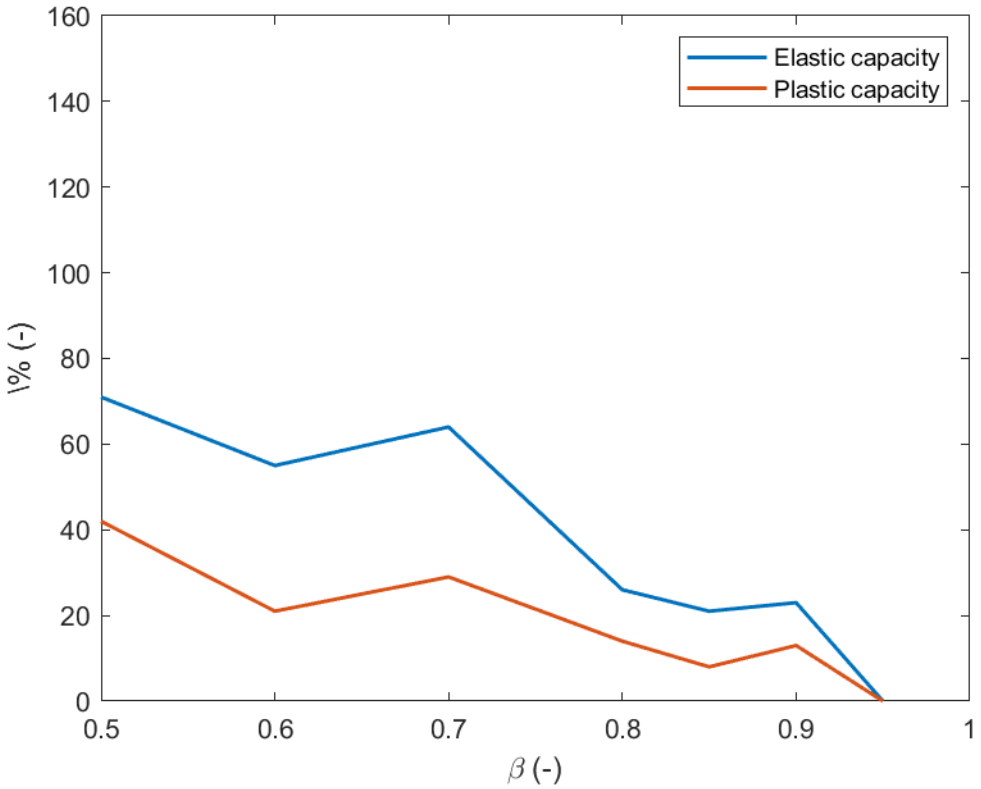

Figure 6.3: Development of capacity loss

The eccentric model will then start to close up on the capacity of the centric model. The result is that the capacity loss between the centric and eccentric placed brace members will shrink. As seen in figure 6.3, the elastic and plastic capacity follow the same pattern, where the only difference is the elastic capacity shrinking faster due to the elastic capacity of the models increasing exponentially.

6.5 Sources of error

When performing a numerical study on a subject, many sources of error can occur. The models used in the primary analysis of this thesis have to be made in the same way to remove unwanted effects or results. The parts used in the analyses can be modelled with the wrong dimensions. If the brace has a larger cross-section than it was supposed to, the rotational displacement will be smaller, and the moment-capacity will be larger than it was supposed to. If the cross-section of the brace is too small, the rotation will increase, and moment-capacity will decrease. If the width of the brace becomes larger, the distance between the brace's webs will become larger, spreading the loads over a larger region on the chord's face. This effect will stop the stresses on the chords from building up and thus reach the ultimate stress after a larger load, giving it a larger moment-capacity. For thinner cross-sections, the stresses will build up quicker, resulting in a smaller moment-capacity.

The chord could also have been modelled wrong. A larger cross-section of the chord will make the chord's face taller, resulting in a smaller needed force to make the

chord's face yield and deform correctly. A smaller cross-section does the opposite, resulting in a larger force needed to yield the face. If the chord is made with the wrong length, effects from the boundary conditions can occur in the joint zone, strengthening the face, thus increasing the moment capacity.

After the analysis has been run, stresses, displacements and forces are extracted. The largest force which can be applied to the structure occurs when an element in the model reaches the ultimate stress. In some cases, it can be hard to point out the location of the ultimate stress node. If the wrong element is located, there is a possibility that another element already has reached the ultimate stress allowed, meaning the force extracted is too large. To calculate the rotation of the chord's face, displacements on the chord face need to be extracted. The maximum displacements occur where the top and bottom flanges of the brace meet the chord's face. If the wrong node is chosen, the rotation would be miscalculated.

When extracting the results, the wanted outputs have to be chosen manually. Manual choosing makes it possible to choose the wrong output. When the outputs are later put through some calculations, the moment or rotation of the structure will become wrong.

The outputs are run through a code which calculates moments and rotations. This code imports the outputs from Abaqus and runs them through a code, plotting the moment-rotation curve. In some cases, the stresses imported from Abaqus have reached the ultimate stress early, leading to a series of higher stresses than allowed. During those stresses, the force keeps growing, increasing moment-capacity and rotation. Points at the tables containing stresses and forces are added to the code to stop the calculations at those points. If the points added are in the wrong area, the forces could either be higher or lower than wanted, making the moment-rotation curve wrong. At the same time, the displacements of the chord face need to be stopped at the same time for the code to assign the right moment to the right rotation. If the wrong points are neglected in either displacements or forces, the wrong moment will be paired with the wrong rotation, leading to a wrong moment-rotation curve.

7 Parameter study

Some simplifications are made to speed up the process when the models are made. In this section, some of the simplifications are changed to investigate the infliction they make on the results.

7.1 Quadratic vs rectangular cross-section

For most of this thesis, the braces have had equal width and height. In this subsection, quadratic and rectangular cross-sections of the brace will be compared to investigate their difference. Another way of putting it, different widths of the brace will be tested when the β-value remains the same. A comparison will be made, using the cross-sections shown in table 21. The results can be seen in figure 7.1.

Chord (mm)	Brace (mm)	$\beta(-)$
200×200 × 8	160×160 × 10	0.80
200×200 × 8	160×80 × 10	0.80

Table 21: Cross-sections of chord and brace when β=0.80

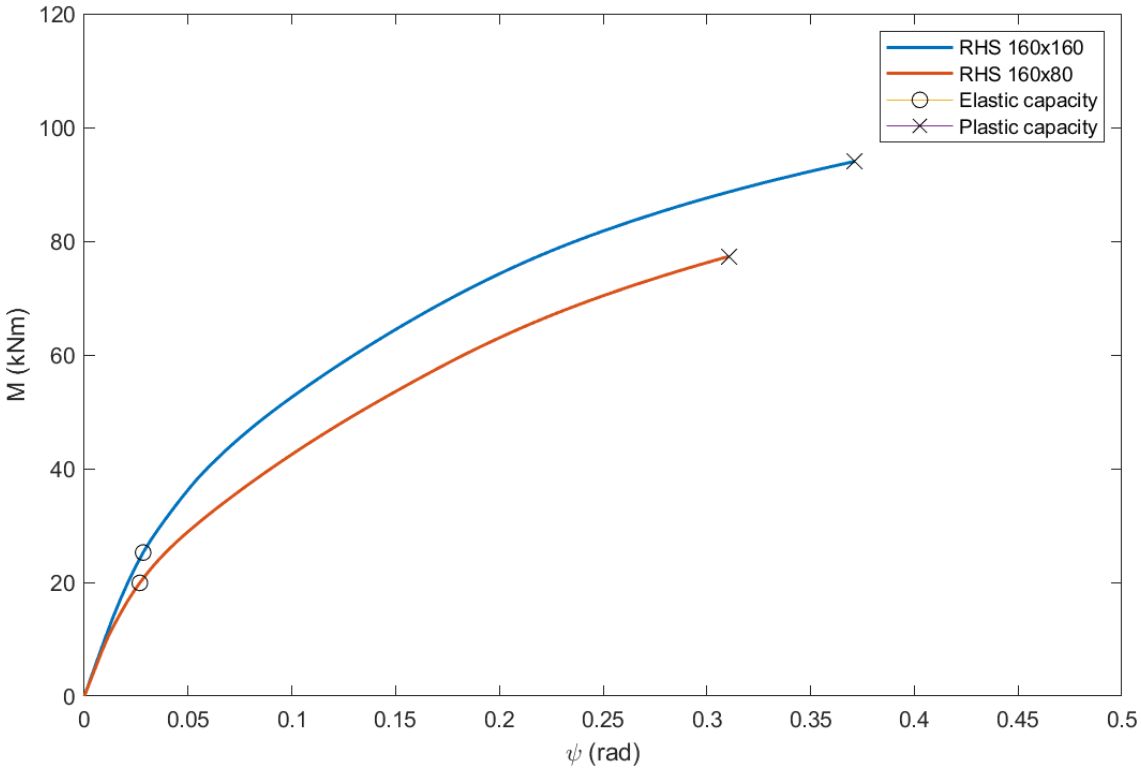

Figure 7.1: Comparison between quadratic and rectangular cross-section

As seen in figure 7.1, both the quadratic and rectangular cross-section behaves mostly the same way. The monotonous behaviour stops when the two cross-sections close up to the elastic moment-capacity. At this point, the quadratic cross-section has a capacity which is 14% higher than the rectangular cross-section. See table 22.

β=0.80	160×160 × 10	160×80 × 10	Capacity loss (%)
Elastic capacity (kNm)	25,3	19,4	23
Plastic capacity (kNm)	94,0	78	19

Table 22: Comparison between quadratic and rectangular cross-section with β=0.80

Entering the plastic region, the curves part ways. Leading to the quadratic cross-section having a higher plastic capacity and maximum rotation of the chord face. The forces are transferred from the brace to the chord through the brace webs. When the width of the brace becomes smaller, stresses on the chord face intersect. The buildup of the stresses in the chord face leads to the stress reaching the ultimate stress earlier.
Figure 7.2a and figure 7.2b shows a quadratic and rectangular cross-section under the same load.

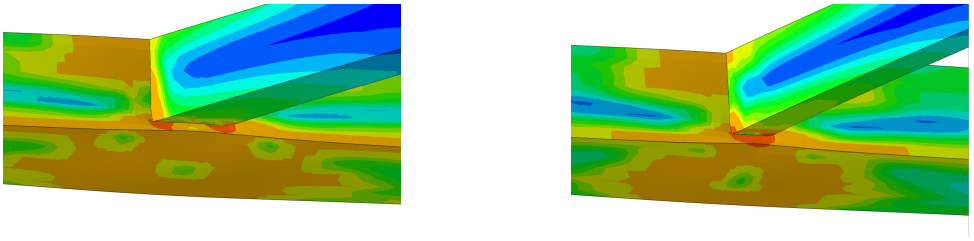

(a) Quadratic cross-section (b) Rectangular cross-section

Figure 7.2: Stress comparisons between quadratic and rectangular cross-section

7.2 Corner configuration

Using sharp corners instead of curved corners was one of the simplifications to speed up the modelling process. Table 23 shows the cross-sectional data used for curved corners. The inner radius $r_i = 1.0t$, and the outer radius $r_o = 1.5t$, where t is the thickness of the profile created.

β=0.80	Cross-section (mm)	$r_i(mm)$	$r_o(mm)$
Chord	200×200 × 8	8	12
Brace	160×160 × 10	10	15

Table 23: Cross-sectional data using curved corners

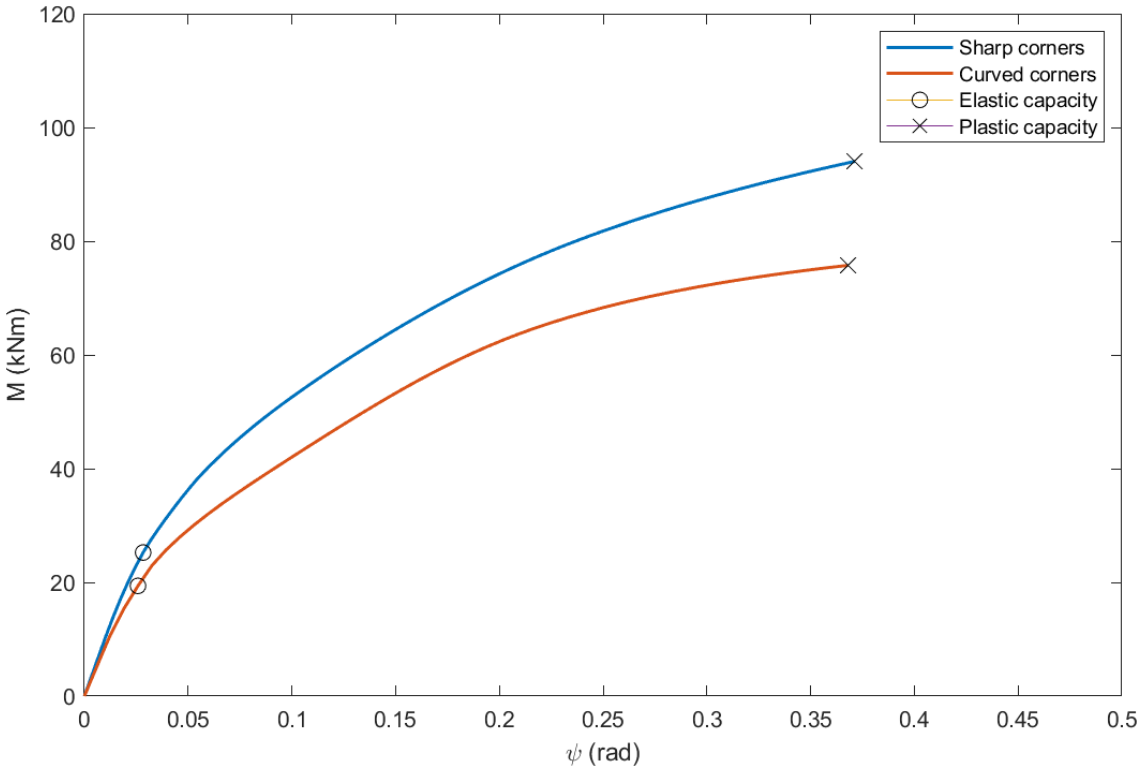

Figure 7.3: Comparison between sharp and curved corners

β=0.80	Sharp corners	Curved corners	Capacity loss (%)
Elastic capacity (kNm)	25,3	19,8	22
Plastic capacity (kNm)	94,0	76,3	19

Table 24: Key results from analysis regarding corner configuration

As both figure 7.3 and table 24 shows, the capacity is higher when sharp corners is used in the models. Initially, the stiffness is almost equal to the point of elastic moment-capacity. The sharp corner model has an elastic moment-capacity of 25,3 kNm, while the curved corner model has 19,8 kNm, 22% lower than the sharp corner model. Post elastic behaviour differs a lot from one another. Resulting in a plastic moment-capacity of 94 kNm for the sharp corner model and 76,3 kNm for the curved corner model, making the capacity loss 19%.

7.3 Thickness of brace wall

Different thicknesses of the brace distribute the forces over different areas of the chord face. Smaller thicknesses transfer the forces onto a smaller area on the chord, giving a local stress collection which can bring the chord to failure. Larger thicknesses distribute the stresses over a larger area, making it possible for the brace to transfer larger loads before reaching stress limits. In this subsection, the thickness of the brace will be changed to investigate how the chord's moment-capacity changes depending on the chosen brace thickness. The thicknesses chosen to be investigated are presented in table 25.

Chord	Brace	β
200×200 × 10	160×160 × 8	0.80
200×200 × 10	160×160 × 10	0.80
200×200 × 10	160×160 × 12	0.80

Table 25: Cross-sections used to investigate impact of brace-thickness

The results from the analyses is presented in figure 7.4.

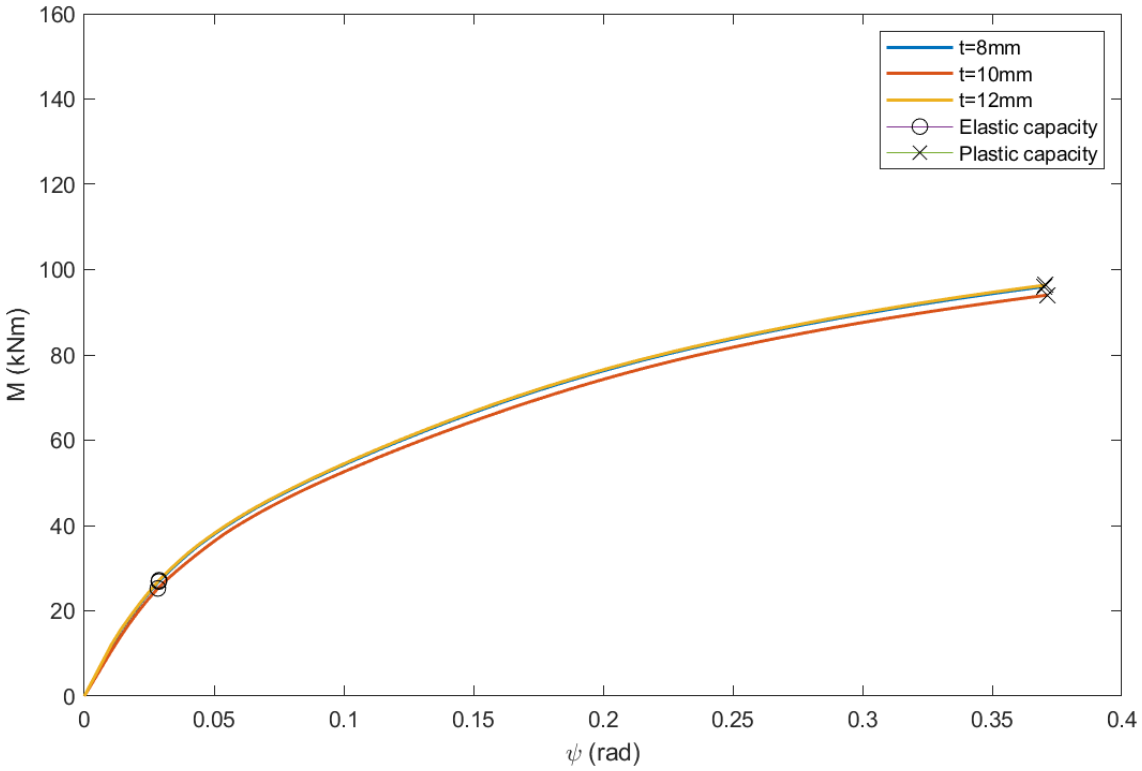

Figure 7.4: Comparison between different brace thicknesses

As seen in figure 7.4, the stiffness of the structure remains almost the same when changing the brace thickness. As mentioned earlier, thicker cross-section will distribute the stresses over a larger area of the chord face. Hence larger loads are needed to increase the stresses to yielding.

8 Summary and conclusion

8.1 Summary

In this thesis, a study investigating the behaviour of eccentrically placed braces on chords subjected to out-of-plane bending moment was performed.

An experimental test and several finite element analyses were performed to investigate how the eccentrically placed brace behaves compared to a model with a centric placed brace. Each analysis had a model where the brace was placed both centric and eccentric. The models were verified by comparing results from the model with the experimental test results and formulas from the Eurocode. When the models had the correct behaviour, the brace was placed eccentrically in relation to the chord's longitudinal centre line. Key values such as elastic and plastic capacity were located as the stresses reached the yield and ultimate stress. The moment-rotation curve for each model was then plotted to investigate how the behaviour differs from each other.

A parameter study was then performed to investigate how some parameters affect the results. Since the models are the same, the parameter study was only applied to the structure where β=0.80.

8.2 Conclusion

- Plasticization of the chord face is the failure mode when $\beta \leq 0.85$ for eccentric placed brace members.
- Plastizication of the chord side wall is the failure mode when $\beta > 0.85$ for eccentric placed brace members.
- The most important parameter when the brace is placed eccentric onto the chord is β.
- For eccentrically placed brace members, the elastic capacity increases exponentially with increasing β, while the plastic capacity increases linearly.
- Calculating the capacity of eccentric placed brace members by using half the capacity of eccentric placed brace members with β equal to the stiffest part is a very conservative method.

8.3 Suggestions to further work

- Further investigation of behaviour of an eccentric placed brace member should be conducted.
- A larger parametric study should be conducted to investigate how different parameters affect the capacity of the structure.

- Design of eccentric placed brace members made of RHS-profiles should be added to Eurocode 3.

Bibliography

Bakker, M. C. M. (1990). *Yield Line Analysis of Post-Collapse Behavior of Thin-walled Steel Members*. Stevin-Laboratory.

Dhatt, G., G. Touzot and E. Lefrancois (2012). *Finite Element Method*. ISTE ltd.

NS-EN 1993-1-8 (2009). *Eurocode 3: Design of steel structures - Part 1-8: Design of joints*. NS-EN 1993-1-8:2005+NA:2009. Oslo: Standard Norge.

Gil, B. et al. (2003). *An assessment of the rotation capacity required by structural hollow sections for plastic analysis*. Swets Sweitlinger.

Larsen, P. K., A. H. Clausen and A. Aalberg (2003). *Stålkonstruksjoner, profiler og formler*. Fagbokforlaget, 3. utgave.

Packer, J. A. et al. (2009). *Design guide for rectangular hollow sections joints under predominantly static loading*. Cidect.

SIMULIA (2011). *Abaqus/CAE user's manual*. Dassault Systems.

Trahair, N. S. (1993). *Flexural-torsional buckling of structures*. CRC Press lac.

Zhao, Bida, Chao Sun and Hui Li (2020). *Study on the moment-rotation behavior of eccentric rectangular hollow section cross-type connections under out-of-plane bending moment and chord stress*. Louisiana State University.

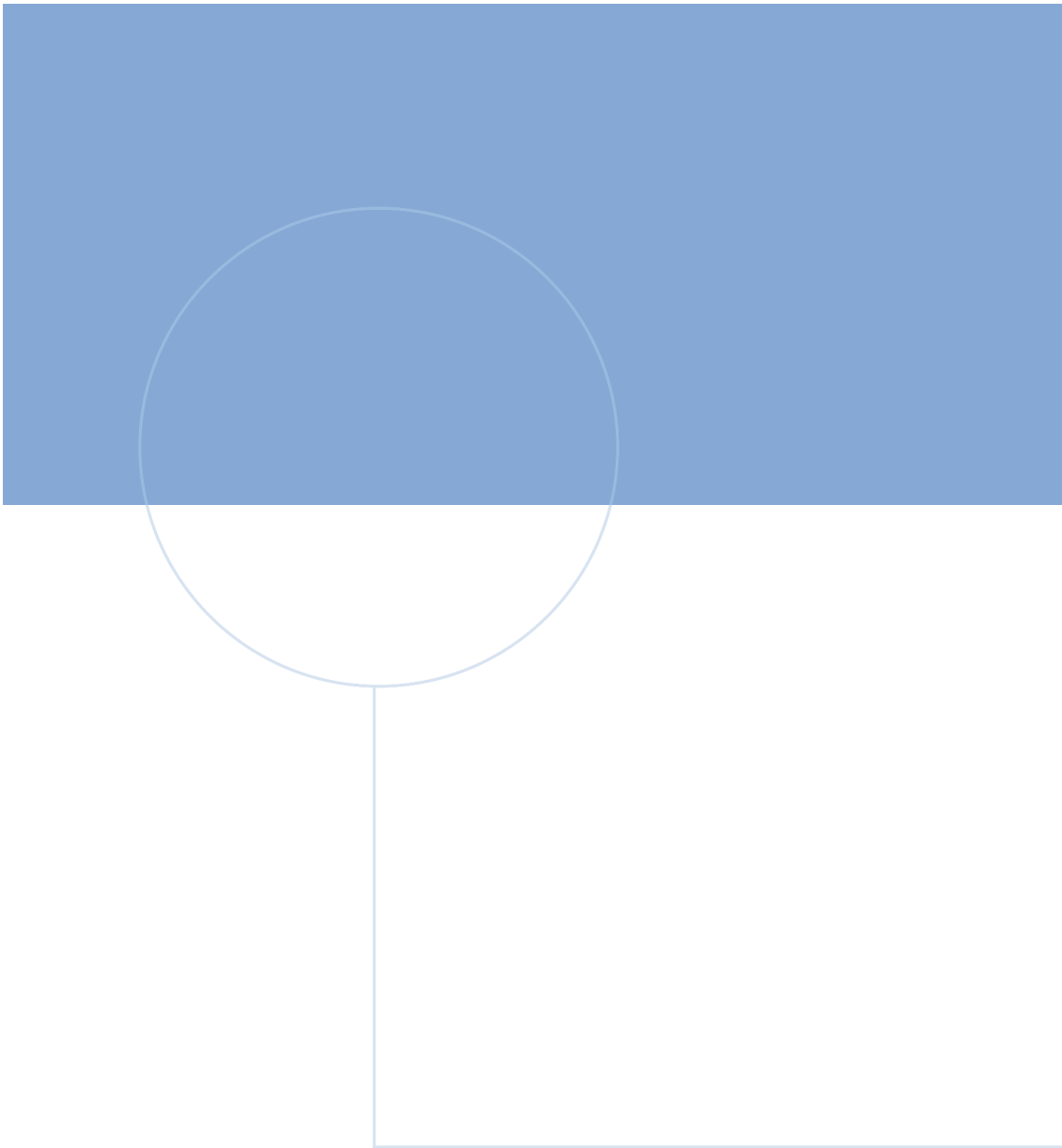

NTNU

Norwegian University of
Science and Technology